

**PREDICTION OF PROCESS-INDUCED DEFECTS BY PLY-DROPS IN THE DESIGN
OPTIMIZATION OF A COMPLEX COMPOSITE LAMINATE.**

by

SITANSHU PANDYA

Presented to the Faculty of the Graduate School of
The University of Texas at Arlington in Partial Fulfillment
of the Requirements
for the Degree of

Master of Science in Mechanical Engineering

THE UNIVERSITY OF TEXAS AT ARLINGTON

August 2017

Copyright © by Sitanshu Pandya 2017

All Rights Reserved



ACKNOWLEDGEMENTS

I would like to express my gratitude towards my supervising professor Dr. Robert M. Taylor, his invaluable support, endless guidance with patience, and motivation made this thesis study possible. I would like to thank Dr. Alex Selvarathinam and Dr. Scott Norwood and for their remarks and guidelines on this work. I express my gratitude to Dr. Wen S. Chan providing material and advice.

Additionally, I would like to thank Dr WOODS, Scott Berggen, and Anirudh Jayan for support in manufacturing and Jo Novak and Blesson Isaac for helped me in MATLAB coding part.

August 3, 2017

DEDICATION

This thesis study is dedicated to Guru Shivanandji and my parents Mr. Harkantray D Pandya and Mrs. Devyani H Pandya, for their unconditional love and support throughout my life.

I would appreciate Deepak Polaki's efforts for guiding and explaining concepts and procedure throughout my research work. I also would like to thank Sanjana Shah, my brothers Chinmay Godbole, Piyush Yadav and Pritish Mandre and many others for their encouragement throughout my academic life.

July 11, 2017

ABSTRACT

Prediction of Manufacturing Defects during Cure Process Induced by
Ply-Drops in the Design Optimization of Complex Composite Laminate.

Sitanshu Pandya, MS

The University of Texas at Arlington, 2017

Supervising Professor: Robert M. Taylor

The objective of this work is to characterize manufacturing process-induced warping defects due to ply drops in composite laminates to guide composite laminate design. Composite laminate optimization seeks weight efficient models, but the process can also generate complex ply geometry, which compounds the challenges of the already rigorous composite laminate manufacturing process. Increased design complexity enhances the likelihood of manufacturing process-induced defects like warping; therefore, it is important to predict such defects in the design phase to make the product more efficient yet producible and thereby avoid such defects. This work study is manufacturing process-induced warpage in complex composite laminates from a three-phase design optimization process that includes composite free size conceptual design ply sizing optimization, and stacking sequence optimization. A mathematical model that could be included in optimization process could help eliminate these defects in the design phase. Consequently, an Analytical model was developed to predict warpage and was compared with experimental and finite element models. The full-size optimized laminate was fabricated, to understand the manufacturing defects for an actual composite laminate. The results obtained from the analytical model correlated with the results of experimental and finite element models. Hence, the mathematical model could be incorporated into the three-phase optimization process.

TABLE OF CONTENTS

Acknowledges.....	iii
Dedication.....	iv
Abstract	v
List of Illustrations	viii
List of Tables.....	x
CHAPTER 1: INTRODUCTION.....	11
CHAPTER 2: BACKGROUND.....	12
2.1 Design Optimization.....	12
2.2.1 Composite Free Size optimization (ply shape optimization).....	13
2.2.2 Composite Size optimization.....	13
2.2.3 Shuffling optimization.....	14
2.2 Composite Laminate Manufacturing Processes.....	15
2.3 Types of Defects Induced due to Manufacturing.....	21
CHAPTER 3: COMPOSITE LAMINATE Design and Manufacturing Study.....	25
3.1 motivation/objective.....	25
3.2 Free-size optimization on optimized composite laminate.....	25
3.2.1 Model formulation.....	26
3.3 Size optimization on optimized composite laminate.....	28
3.4 Shuffling optimization on optimized composite laminate.....	29
3.4.1 Buckling Criteria.....	29
3.4.2 Manufacturing Criteria.....	29
3.4.3 Validation of stacking sequence.....	30

3.5 Editing Finite Element Model to CAD model.....	31
3.6 Manufacturing.....	34
3.7 Manufacturing induced defects.....	38
CHAPTER 4: Warpage Prediction Models.....	39
4.1 Analytical Model for predicting Warpage due to cooling cycle in cure process	39
4.2 Experimental model - Fabricating coupons	43
4.3 Finite Element Modal for predicting warpage due to cooling cycle in cure process.....	45
CHAPTER 5: Warpage Prediction Results	49
5.1 Analytical Model for predicting Warpage due to cooling cycle in cure process.....	49
5.2 Experimental model - Fabricating coupons.....	51
5.3 FEM modal for predicting Warpage due to cooling cycle in cure process.....	54
5.4 Comparison Results.....	58
CHAPTER 6: CONCLUSION and FUTURE WORK.....	59
APPENDICES	
A. FEM file structure for shuffling optimization.....	61
B. MATLAB CODE.....	69
C. FEM FILE STRUCTURE for Coupons.....	75
REFERENCES.....	78

LIST OF ILLUSTRATIONS

Figure 1: Three phase optimization process.....	12
Figure 2: Autoclave in composite lab, Mae dept., uta.....	16
Figure 3: Oven with vacuum lines and thermocouple.....	17
Figure 4: Compression heat molding machine, utari.....	18
Figure 5: Laminate geometry	26
Figure 6: Ply-drop schematic.....	30
Figure 7: Optimized stacking sequence.....	30
Figure 8: Unedited ply shapes	31
Figure 9: Hypermesh GUI command for ply smoothing and surface generation	32
Figure 10: Edited ply shapes	33
Figure 11: Ply arrangement for cutting through nesting process	34
Figure 12: Ply cutting at 45°	35
Figure 13: Ply shapes of carbon fiber tapes	35
Figure 14: Lay-up process, release film, and breather	36
Figure 15: Vacuum bagging	37
Figure 16: Demo cure cycle of Hexcel im6/3506-1.	38
Figure 17: Cured laminate with warpage	38
Figure 18(a): Actual ply-drop intersection FBD	39
Figure 18(b): Modified ply-drop intersection FBD	39
Figure 19: Schematic of analytical model	40
Figure 20 (a): Coupons before cure	44
Figure 20 (b): Coupons after cure	44
Figure 21: Coupons with restricted edges.....	45
Figure 22: Boundary condition: Roller support at the end.....	48

Figure 23: Command in HyperMesh for material orientation for 3d elements	48
Figure 24: Deformation results based on the analytical model for 0.....	49
Figure 25: Deformation results based on the analytical model for 90.....	50
Figure 26: Deformation results based on the analytical model for -/+45.....	50
Figure 27: Trends of change in angle of with ply-drops and the orientation for Analytical model.....	51
Figure 28: 0° Orientation layup with 16 ply-drop	52
Figure 29: -/+45° Orientation layup with 16 ply-drop	52
Figure 30: 90° Orientation layup with 16 ply-drop	52
Figure 31: coupling effect for a classical lamination theory.....	53
Figure 32(a): Coupons with restricted edges after cure.....	53
Figure 32 (b): Moment at ply-drop intersection.....	54
Figure 33(a): 0° plies with 16 ply-drops	55
Figure 33(b): 0° plies with 16 ply-drops 100x exaggerated.....	55
Figure 34(a): 90 plies with 16 ply-drops	56
Figure 34(b): 90° plies with 16 ply-drops 100x exaggerated	56
Figure 35(a): -/+45° plies with 16 ply-drops.....	57
Figure 35(b): -/+45° plies with 16 ply-drops 100x exaggerated	57
Figure 36: Trends of change in angle of with ply-drops and the orientation for FEM.....	58
Figure 37: Comparison of FEM and Analytical results.....	59
Figure 38: Z-displacement for composite laminate after thermal loading.....	60
Figure 39: (a) Ply slope effect on larger panel (b) Ply drop effect on smaller panel.....	60
Figure 40: Cross-sectional view of optimize composite plate.....	61

LIST OF TABLES

Table 1: List of consumables material used during hand layup process.....	18
Table 2 : Generic composite material properties.....	26
Table 3: Generic carbon fiber/epoxy tape material system maximum strain criterion allowable.....	27
Table 4: Generic carbon fiber/epoxy tape material system constant value bearing and bypass Allowable.....	28
Table 5: Material properties of IM6/3506-1 for analytical model.....	41
Table 6: Experimental model for different combination ply-drop and orientation.....	43
Table 7: Experimental model for different combination ply-drop and orientation with restricted edges.....	45
Table 8: FEM model for different combination ply-drop and orientation.....	46
Table 9: Material properties for IM6/3506-1 prepreg.....	46
Table 10: Material properties for 3506-1 resin system.....	47

1. Introduction

Design and Manufacturing of composite structures have been a challenging and time-consuming process. Composite structures are weight efficient when compared with other engineering materials used in industries, but the cost is a major factor for using composites structures. Therefore, there are a need for more efficient weight, and material saving designs methods. Design Optimization is one of the ways to achieve this objective. As the variation of material is bi-directional regarding mechanical properties of composites, the optimization process is more complex with some possible design solutions out of which to choose correct solutions, is complicated decision-making process by achieving all objectives. Hence a new approach was developed by Altair suggested by Ming Zhou, Raphael Fleury, and Martin Kemp² which is cost saving and efficient for composite structural optimization. This three-phase optimization process gives a weight efficient design, but also the results have some complex ply geometry which makes manufacturing more challenging, and the finished product would be unpredictable. In this thesis study, the aim is to develop a mathematical model to include that in design optimization phase to avoid this defect. Hence, an Analytical model was developed based on the classical lamination theory for the ply-drop intersection, and the results were compared with experimental and finite element model to validate the results from the analytical model. The full-size composite laminate was fabricated. The uniqueness of this study is on the focus on deformation of the complex composite laminate produced during cure process due to series of ply-drops within the laminate.

2. Background

This thesis study is a continuation of “COMPOSITE PLATE OPTIMIZATION WITH STRUCTURAL AND MANUFACTURING CONSTRAINTS by Deepak Polaki, supervised by Dr. Robert Taylor. In continuation to this study shuffling optimization was performed on the optimized composite laminate after free-size and size optimization. The laminate was manufactured, and a detailed study of manufacturing induced defects due to uneven thickness was carried out in this thesis. This section helps to relate and understand the research done previously.

2.1 Design Optimization

Design optimization of the isotropic structure is simple compared to composite structures optimization. As composites are heterogeneous, material properties vary in the multiple-coordinate system and considering these changes; an optimization process has to generate a best possible shape, size and stacking sequence for plies within composite laminate¹⁸. Three phase optimizations of the composite structure are popular in the aircraft industry. Phase I focuses on generating ply shapes through Free-Size optimization; Phase II further improves the number of plies for a given ply layup and regulates the individual ply thickness along with total laminate thickness: Then Phase III finalizes design details through Stacking sequence optimization satisfying all manufacturing and design constraints².

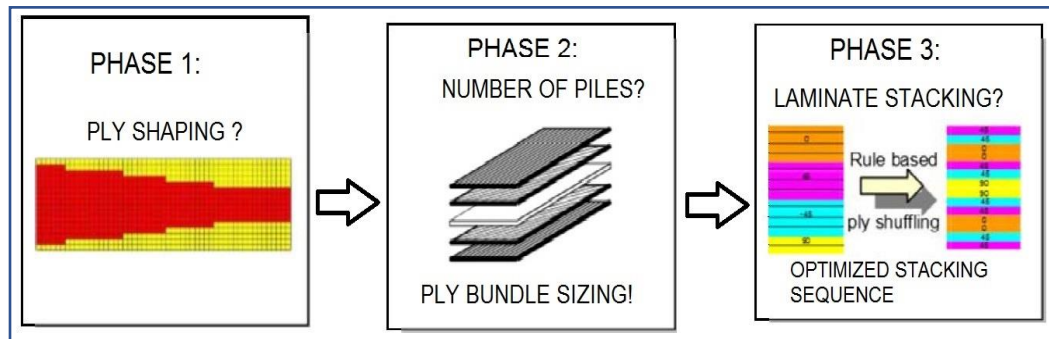


Figure 1: Three phase optimization process²

In 2014, Taylor R. et al., considered a laminate with a rectangular cut out with one hole with practical design constraints, studied, compared weights, and manufacturability through various optimization methods^{27,28}. Orthotropic composite structures require a higher level of tooling and additional processes at the conceptual level. Design and manufacturing constraints are implemented at the system level, and stacking sequence optimization is applied at the detail level to formulate the final design of the structure.

2.1.1 Free Size Optimization

Free size optimization uses the thickness parameter as a size parameter and offers a direct fix for the precision problem in the shell elements. Thus, creating topological- style optimization result. However, this type is restricted to only isotropic materials; a generalized process can be used for the composite materials.

This phase uses the outer boundary of the plies to modify the problem. Various grid locations are allocated to the outer part of each ply based on applied loading conditions by satisfying all constraints and achieving the objective to create optimal ply shapes. M.Pohlak et al...³⁰ and Polaki D¹ have used free size optimization in a multi stage criteria optimization of large plastic composite parts.

2.1.2 Composite Size Optimization

After topology/shape/free size optimization gives out the best possible shape, the size optimization deals with attributes of elements such as shell thickness, beam cross-sectional properties, spring stiffness, and mass. These attributes are redefined and controlled according to design variable and constraints are satisfied during the optimization process. In general, the objective is to minimize weight by optimizing elements along the thickness and working on the overall thickness of the laminate. The variable thickness could be possible depending on boundary condition with different load cases.

2.1.3 Shuffling Optimization

H Ghiasi, K Fayazbakhsh, D Pasini, L Lessard¹⁹ developed optimization algorithms in constant stiffness design. Different parameterization and optimization algorithms were briefly explained and compared the advantages and shortcomings of each algorithm to get optimal stacking sequence. Pagano, N. J., and R. Byron Pipes²⁰ presented an approach to predict the exact stacking sequence of specific orientations which leads which makes design safe against delamination under uniaxial static and fatigue loadings.

The use of lamination parameters is another approach to represent the in-plane and flexural stiffness in the optimization of laminated composites. Tsai first used the optimization of composite laminate²¹ and later applied to the buckling optimization of orthotropic laminated plates by Fukunaga, Hisao, and Hideki Sekine²² of laminated composites.

The composite shuffling optimization step of the three-phase composite design optimization determines optimal stacking of the plies to meet manufacturing requirements. It is important to understand stacking sequence in a composite laminate product.

Though the design achieved after Phase II optimization contained all ply layout, specific manufacturing constraints are not satisfied. Therefore, stacking sequence of individual plies is being shuffled during this period to satisfy production constraints while keeping all design constraints intact.

Some other manufacturing constraints are enforced: (a) limit on consecutive plies of the same orientation (b) pre-defined cover lay-ups; (c) pre-defined core lay-ups.

2.2 Composite Laminate Manufacturing Process

The manufacturing process involves adding reinforcements to the resin system which could be a final form of product or need to be prepared for the final product. Process and tooling affect composite properties. Therefore, detailed knowledge of manufacturing is required when designing composite parts.

There are two parts involved in manufacturing composite laminates: lay-up and curing. The various process by are known for manufacturing as explained below:

1. Hand layup

The traditional and most commonly known technique is laying up composite plies into the mold by hand. This method is used where there is less accuracy required. It's labor intensive and time-consuming, but hand layup can eliminate the initial cost and maintenance cost of complex machinery needed in a technique like ATP and AFP.

a. Wet layup

In this type of process both resin and fiber are separate. Fibers are in the form of dry fabric or unidirectional tapes or strands. The resin used in this kind of process is two part epoxy thermoset resin. The first layer of resin is coated on mold, fibers are placed, and successive layers of fiber and resin are coated on one another. The number of layers of fiber are based on design. At the end the layup, part is subjected to the curing process.

b. Prepreg Layup

Fibers are pre-impregnated with a resin system. This type of prepreg fibers lay-up could be done directly on mold and could be subjected to the curing process.

The curing process depends on resin system used in manufacturing. It involves vacuum, high pressure, and temperature, and following are some common methods used for the curing process:

a. Autoclave

The most common method used in the curing process is an autoclave, which is a pressure vessel chamber that has a heating system and can hold vacuum as shown in the picture below. The size of the autoclave, the range of temperature, and pressure can operate on the curing system of resin which varies from application to application.



Figure 2: AUTOCLAVE in COMPOSITE LAB, MAE dept., UTA

b. Out of Autoclave

This process is used when there is no pressure, or little amount of pressure is required to cure the resin system. A typical heat Oven with thermocouple and vacuum lines could be used for this process. This type of curing is less accurate

and can affect the final strength of the material. LW Davies, RJ Day, D Bond, A Nesbitt, J Elli²³ presented a cure cycle study, an out-of-autoclave toughened resin film infusion process as part of the examination of an alternative manufacturing process for composites. They showed that cure cycles with a relatively short dwell time and higher heating rate compared to an autoclave cure led to enhanced flow properties of the toughened resin system. High-quality laminates, comparable to autoclave panels, were manufactured with vacuum pressure only by modifying the original vacuum bagging arrangement.



Figure 3: Oven with vacuum lines and thermocouple, IPPM, UTARI

c. Compression heat molding.

This type of curing is used where high temperature curing systems are required like curing amide based resin or ceramic based composites. The heat is supplied from two hot plates with a sealed chamber to hold vacuum and pressure is applied by controlling compression between the plates. There is enormous initial and maintenance cost involved with this kind of process, but it gives accurate results.

The limitation with this process is it can only cure flat laminates with even thickness.



Figure 4: compression heat molding machine, IPPM, UTARI

Hand lay-up and curing is done, certain consumable materials are required throughout the process. The following table explains each term and its uses:

Peel-ply	A sacrificial open weave fiberglass or perforated heat-set nylon ply placed between the laminate and the bleeder/breather to provide the textured and clean surface necessary for further lamination or secondary bonding.
Breather cloth	The fiber volume fraction, and hence mechanical properties, can be improved by bleeding off excess resin. To achieve this, a polymeric film sealed to the mold edges encloses the laminate. A porous material used to provide a gas flow path over the laminate both to permit the escape of air, reactants, moisture, and volatiles and to

	ensure uniform vacuum pressure across the component. It may also act as the bleeder cloth.
Release film	A (perforated) sheet of material placed between the laminate and the mold surfaces to prevent adhesion.
Caul plate	A mold or tool set on top of the laminate inside the bag to define the second surface.
Bagging film	The plastic film which can hold vacuum within the bag.
Tacky tape	Adhesive strip used to bond the bag to the tool and provide a vacuum seal.
Breach unit	A connector through the bagging film to permit a vacuum to be drawn.
Vacuum pipes	The link between the breach unit and the vacuum pump.
Vacuum pump	A high-volume pump (absolute vacuum is rarely required) suitable for continuous running. For some slow-curing epoxy resins, twenty-four operation may be needed.
Pressure gauges	Clock-type or digital gauges attached via a breach unit connection.
Vacuum bagging	A breach unit penetrates the bag and permit a vacuum to be drawn in the bag. This imposes a consolidation pressure of up to ~1000 mbar on the materials in the bag. The principal disadvantage of this technique is the disposable materials that are included in the bag

Table 1: List of consumables material used during hand layup process^{32,33}

2. Automatic Tape Placement(ATL):

The fabrication from ATL will be best suited for lay-up of complex ply shapes. ATL systems were conceived from the end of the 1960s onwards⁸. The earliest known reference to an ATL is a patent under the name of Chitwood and Howeth⁹ in 1971, describing a method of laminating composite tape onto a rotatable base-plate using Computer Numeric Control (CNC). In 1974 Goldsworthy¹⁰, described an automated system delivering 76 mm wide tape over a curved surface where the head was able to rotate and withhold material to improve the part complexity that could be manufactured using ATL layup.

Tape laying is a computer-numerically controlled (CNC), usually, employs a Cartesian coordinate system positioning with rotational freedoms. It may be used for thermoset or thermoplastic matrix composites. This technique can do lay-up of flat or low curvature surfaces accurately, but accuracy decreases with complex geometry. It is often associated with high-quality aerospace composites such as flight control surfaces and wing skins. The process has high initial and running cost, which makes its use limited to the high-cost products.

3. Automatic Fiber placement(AFP):

AFP systems were commercially introduced towards the end of the 1980s, and were described as a logical combination of ATL and Filament winding¹¹; by combining the differential payout capability of Filament winding and the compaction and cut-restart capability of ATL. Several of the lessons learned during the development of ATL, such as roller design and material guiding were incorporated into these AFP systems, and as such, they were immediately available from commercial suppliers.

Process in which a multi-axis robot assisted wet-wind yarn or roving around a series of pins in a predetermined pattern is done. The restraints around which the fibers are wound permit the construction of parts without the limitations of geodesic paths. The process is perhaps more applicable to thermoplastic matrix composites where online consolidation and cooling allow its use without the requirement for the fiber restraints. Automated fiber placement (AFP) uses pre-impregnated tows to build up a component against a mold or mandrel surface. The narrow tows allow more complex parts to be manufactured than when using automated tape laying. This type of process is often preferred in the geometry with junctions and sudden change in contour.

2.3 Types of Defects Induced due to Manufacturing

There are different kinds of defects caused during manufacturing process due to improper tooling, inappropriate layup, Inclusions, Improper care, improper machining or difference in CTE. Following are some defects induced due to fabrication process:

1. Voids and porosity

Voids and porosity are some of the unavoidable defects in a composite laminate. They are formed primarily due to the mechanical air entrapment during the lay-up and moisture absorbed during the material store. The inclusion of voids affects mechanical properties of the composite laminate. Ling Liu, Bo-Ming Zhang, Dian-Fu Wang, and Zhan-Jun Wu⁵ investigated the effects of pressure conditions on the void contents and mechanical properties and proved that the results suggest that both the strength and modulus decrease with increasing porosity. A higher void sensitivity for ILSS, flexural

strength and flexural modulus were obtained, and tensile strength decreases relatively slowly, while the tensile modulus is insensitive to the void content.

2. Tool marks and excess resin

This kind of defects is common due to improper handling of part and material. The tool makes, and excess resin initiates the delamination at the surface and the resin pocket causing part failure in services. Resin pockets could be avoided by following standard manufacturing procedures and proper work practices. Some this is mentioned in the handbook of composite fabrication⁶.

3. Waviness

Waviness in composite laminate occurs as layer waviness which is characterized by undulation of layers in the direction of thickness. This type of defect affects the compressive strength of the laminate. Daniel and Hyer⁷ investigated for the compressive loading strength of laminate with waviness; experimentally they found the strength of laminate was reduced up to 36% for specimen with severe waviness geometry

4. Ply overlaps and gaps

Intra-ply overlaps and gaps can be included in both type of lay-up, either hand lay-up or automated lay-up. This overlap created a geometric discontinuity resulting into induced residue stress causing unwanted deformation. Sawicki and Minguet¹² carried out simulations and experiments and concluded, this type of defects causes waviness resulting into reduction in compression strength.

5. Warpage

Most of the defects could be eliminated by adopting good manufacturing practices, but some of the defects are due to the nonconventional behavior of

a material which causes undesirable changes in the finished product. This type of defects could not be eliminated, but if this effect could be predicted then its effects could be controlled¹².

In 1974, Chamis, C. C.⁵ proposed a theory that with one fiber of misalignment, and 3 of fiber misalignment was enough to cause warpage. Robert R. Johnson, Murat H. Kural, and George B. Mackey¹³ took the initiative to comprehend the thermal expansion data for several composites material. Also, the report discusses the tuning laminate to achieve zero CTE. This work leads to the research to eliminate warpage during the manufacturing process. An analytical model was developed by Zhenyi Yuan, Yongjun Wang, Xiongqi Peng, Junbiao Wang, Shengmin Wei³¹ and demonstrated that warpage is enhanced linearly with the increase of interfacial shear stress also could predict the part processing deformation. E. Kappel, D. Stefaniak, T. Sprowitz, C. Hühne¹⁵ could predict warpage properties of different prepreg – tool–material combinations. A more focused research was by Gayen, Debabrata, and Tarapada Roy⁴ who developed an analytical model for calculating hydro-thermal stress for tapered composite laminate. They observed that effects of stacking sequence, fiber orientation, the coefficient of thermal expansion (CTE) and coefficient of moisture expansion (CME) have significant roles in the change of inter-laminar shear and axial in-plane stresses distribution through the laminate thickness. JM Svanberg ¹⁶ worked on prediction on manufacturing induced shape distortions and concluded, when a thick component is cured, the conditions are no longer isothermal owing to heat generated by the exothermal cure reaction.

Causes of warpage could be summarized as:

1. Difference in CTE of part and tool
2. Unsymmetrical or unbalanced layup or improper layup.
3. Uneven cooling causing uneven shrinkage through thickness
4. Discontinuity in geometry and material i.e. ply-drop

From the above-stated objects first three could be minimized by selecting tool with a same value of CTE or in an allowable range of difference¹⁴. Ply-drops are decided in the design phase and have an unpredictable effect on the post cure process as there is singular stress built up at the point of material and geometry discontinuity as discussed by Varughese, Byji, and Abhijit Mukherjee²⁴. H Abdulhamid, C Bouvet, L Michel, J Aboissi re presented²⁵ an experimental study of low-velocity impact response of carbon/epoxy asymmetrically tapered laminates. Type and localization of damage were analyzed through C-scan and micrographs. The effects of some tapering parameters and concluded that presence of material discontinuity due to the resin pocket affects less the damage mechanism than the structural difference between the thick and the thin sections.

As discussed by R Haynes, J Cline¹⁵, Classical laminated plate theory is not able to predict Warpage during manufacturing accurately. In thin laminates, convex up curvature can be observed but even in thicker composites, measurable warpage does exist due to under assumption of reference from the plane of symmetry. Such shape distortions surface leads to a greater knockdown in the strength of the composite structure. Throughout much of the manufacturing industry, the solution to component warpage is an iteration of tool geometry until the final distorted composite part matches the design shape. However, the resulting tooling is then not an exact duplicate of the part and is unlikely to yield parts of correct form if the composite constituent materials or processing parameters are changed.

3. Composite laminate design and manufacturing study

3.1 Objective

This thesis concentrates on understanding the bridge between design and manufacturing of composite laminates. After considering all design and manufacturing constraint in design & optimization phase, there are defects induced due to the manufacturing process in the final product. It is important to understand reasons for this undesirable behavior of laminate after manufacturing. Hence, the previous research¹ was followed and the model, which had optimized for free size and size optimization, was subjected to shuffling optimization.

3.2 Free-Size Optimization of Composite Laminate

The aim of the previous study¹ was to design a rectangular laminate with a hole, with maximum compliance and minimum mass. Free size optimization decided the layout to make the laminate with the greatest compliance and work on the in-plane geometry of ply and overall laminate. PCOMP card was used to give the shell element a composite behavior. The layup was assumed as a symmetric smear, and default ply bundle number was used. No slope, 0.10, 0.05 were three different cases considered for total slope value. dummy pressure loads were applied as 0, 1, 2, 3 psi magnitudes were create to obtain buckling resistant shapes,. The objective was to minimize compliance by constraining volume fraction up to 40 %.

3.2.1 Model Formation free size

Geometry with load conditions

The laminate is 10 inches by 20 inches with unidirectional fibers on piles of $[0^0/\pm 45^0/90^0The]$ family that has a centrally located hole of 1.75-inch diameter as shown in figure 5.

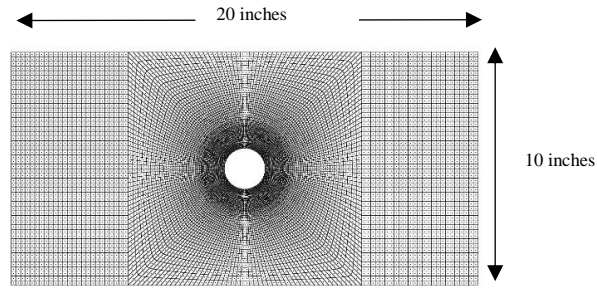


Figure 5: Laminate Geometry¹

Tension, compression, and shear load were applied as distributed point loads along the fastener locations that are spaced with 0.25-inch fasteners at the 5d pitch. The magnitude of compression and tension loads are 20,000 lb/in^2 and magnitude of 10,000 lb/in^2 for shear load.

Material

Unidirectional carbon fiber/epoxy tape with the properties shown in Table 2. An 'MAT8' orthotropic material in Altair Optistruct is used as a material property on the laminate.

<i>Property</i>	<i>Value</i>
E_1	20,000,000 <i>psi</i>
E_2	1,000,000 <i>psi</i>
G_{12}	800,000 <i>psi</i>
G_{23}	500,000 <i>psi</i>
ν_{12}	0.30
t_{ply}	0.01 <i>in</i>
ρ	0.06 lb/in^3

Table 2 : Generic composite material properties

Acreage Strength Criteria

The objective of shuffling optimization is to minimize the mass and generate optimal stacking sequence of the laminate. The structural criteria were assigned as constraints. Static strength and damage tolerance are constrained using strain limits in max strain failure condition and are mentioned in table 3.

Allowable	Value
X_T	$2.5 \times 10^{-3} \text{ in/in}$
X_c	$2.5 \times 10^{-3} \text{ in/in}$
Y_T	$0.2 \times 10^{-3} \text{ in/in}$
Y_c	$0.4 \times 10^{-3} \text{ in/in}$
S	$0.4 \times 10^{-3} \text{ in/in}$

Table 3: Generic carbon fiber/epoxy tape material system maximum strain criterion allowable

Bearing – Bypass Criteria

The bearing and bypass constraints were enforced at fastener locations. These limitations were defined at two end points at fastener locations that captured peak loads which cover fastener locations. The bearing stresses were calculated based on Deepak Poliaki's thesis study¹.

ϵ_{lim} is shown as the upper allowable boundary and is the tensile constraint used in the bearing land region in the optimization.

Allowable	Value
Compressive Bypass Strain, ϵ_{bypC}	$4.2 \times 10^{-3} \text{ in/in}$
Bearing Cutoff stress, F_{Brg}	80 ksi
Linear Interaction Strain, ϵ_{int}	$2.9 \times 10^{-3} \text{ in/in}$

Table 4: Generic carbon fiber/epoxy tape material system constant value is bearing and bypass allowable.

3.3. Size Optimization

In HyperMesh the output card sets up a model for size optimization after free size optimization. It is necessary to customize the design and add extra parameters and criteria to it to run the model

Additional plies are generated as fastener ply bundles and added to the stacking sequence to replace the additional element in fastener region. The design variables were defined, and design variable relationships were set up with respective plies. To find the best possible combination global search option (GSO) is used with DGLOBAL card. To setup, the model further pressure load collector and load step were deleted. The objective and constraint were deleted and the new objective was created as minimum mass. All the 12 models from Free-size optimization were subjected to Size optimization for different total drop value ranging from 0.01 to 0.09. All these models were then compared based on the mass trends, and percentage violations of manufacturing and design constraint. Model with best results was taken and subjected to shuffling optimization.

3.4 Shuffling optimization on optimized composite laminate

The best model was selected from the previous study¹ with pressure load 2, total slope 0.05 and total drop 0.06. The output card sets up the model but just like the last step we need to edit the model. All other design variables except DCOMP, which is to be a design variable for shuffling step optimization, are to be deleted. All the design relationship variables and design equation must be deleted as there is no need of any of those equations. The objective is to minimize mass with the aim to find optimal stacking sequence with Design variable DCOMP. Manufacturing constraints include limiting maximum successive ply-drops up to 4, and the cover which is pre-defined stacking sequence which remained unchanged. The cover constraint is needed after optimization to avoid possible edge effects, and the comp is defined. The responses are the same as that of size optimization, that is, mass, buckling, maximum strain, minimum strain, and CFailure. Out of which buckling, maximum strain, minimum strain, and CFailure is constrained.

3.4.1 Buckling Criteria

The previous study¹ developed Static structural stability by limiting lower limit on buckling eigenvalue during sizing optimization. The procedure to generate ply shapes is more resistant to buckling failure. In optimization process, the buckling eigenvalue is constrained to be greater than 1.02 for the compression and shear load cases.

3.4.2 Manufacturing Criteria

Two manufacturing criteria are applied as constraints:

- Maximum successive ply-drop
- Cover plies of laminate

In actual practice, there are no more than four plies terminated at once, with the aim to minimize the size of resin pockets formed due to ply-drop as shown in figure 6 below:

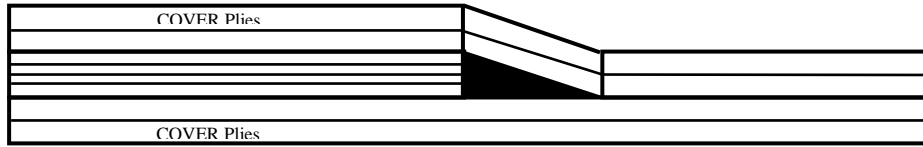


Figure 6: Ply-drop schematic

These resin pockets create material and geometric discontinuity due to which interlaminar stress are introduced within the plies resulting into delamination. Hence, the number of plies dropped are controlled to minimize the size of resin pocket.

Cover plies are stacked as [-45/90/45/0] to avoid a sudden change in orientation, to maintain dimensional stability, and to prevent edge effect. As these kinds of layups are symmetric and stable, hence, eliminates any local unbalanced induced forces.

3.4.3 Validation of stacking sequence

Stacking sequence was validated by checking whether it satisfies the following rules⁴:

1. The layup should be balanced and symmetric.
2. At least 10% of all orientation should be present i.e. at least 10% of 0, 90, 45, -45.
3. No more than four plies of same orientation should be stacked together
4. Place 0 and -/+45 as far as possible from the neutral axis.
5. Place -/+45 plies to cover laminate to avoid low-speed impact.
6. Avoid external ply-drop. Ply-drop should be symmetric, and the distance between successive ply-drop should be 10 -15 times of that of ply-drop.

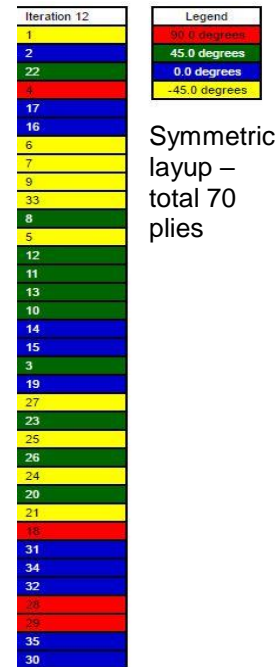


Figure 7: Optimized stacking sequence

3.4 Editing FEM model to CAD model

CAD GEOMETRY EDITING

After stacking sequence, it's important to have ply shapes for manufacturing. Figure below shows ply shapes after shuffling optimization; the spikes at the edges are elements generated by mesh and would be tough to cut. Hence, ply smoothing process was followed to obtain smooth contours for easing the ply cutting process and minimize material loss.

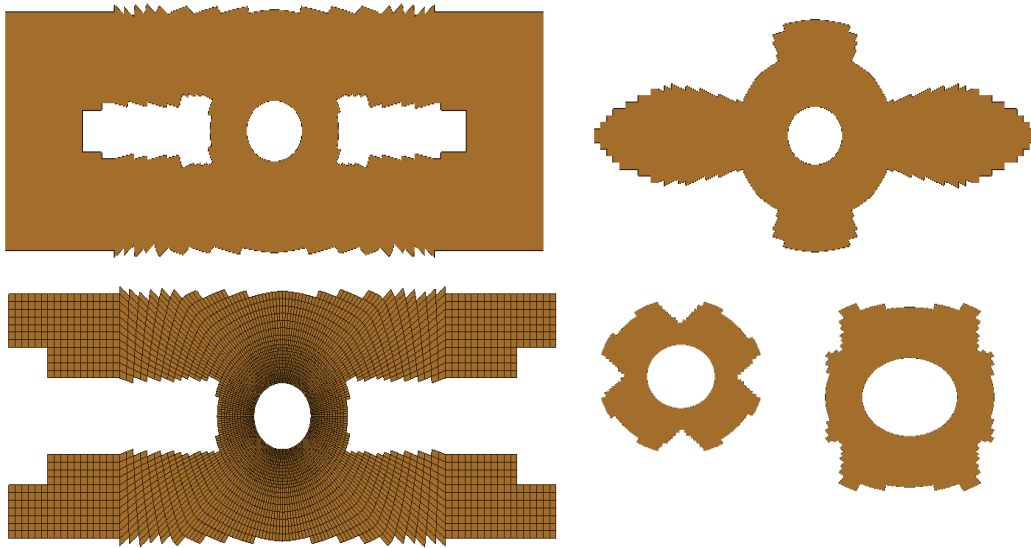


Figure 8: unedited ply shapes

STEP 1: Ply smoothing and surface generation

There is a command in HyperMesh GUI to perform ply smoothing process and generate lines and surfaces for the plies simultaneously.



User profile-> Engineering solutions ->Aerospace->composites->ply smoothing

Following parameters were used to generate smooth surface

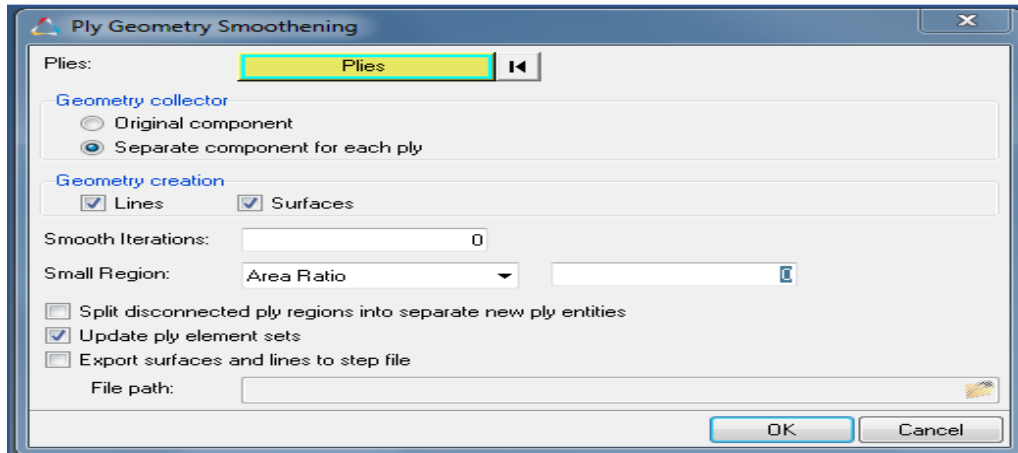


Figure 9: HyperMesh GUI command for ply smoothing and surface generation

The iteration was smoothing the ply shapes with splines and curves which were hard to edit in further steps for creating a manufacture-able shape hence the number of iteration was set to 0.

Step 2: EXPORT STEP FILE TO SOLIDWORKS

After ply smoothing process, surfaces were generated for each ply of the laminate.

Go to Export-> Geometry ->

Step 3: Edit plies surface in SolidWorks based on rules¹ as shown below:

1. Holes or gaps along the fiber direction
 - If hole or gap is less than 100% of tow length requirement, then elements are added to fill area
 - Fill holes, if drilling holes are possible in post manufacturing stage.
2. Tow dimensions along the fiber direction—0° and 90° plies
 - Must be greater than 2" (fiber direction) x 0.50" (transverse direction)

- If tow dimension is less than 50% of tow length/width requirement, then elements within area are removed
 - If tow dimension is greater than 50% of tow length/width requirement, then elements within area are added until minimum dimension requirement is satisfied
3. Tow dimensions along the fiber direction— $\pm 45^\circ$ plies
- Must be greater than 2" x 2" to ensure balance constraint enforced
 - If tow dimension is less than 50% of tow length/width requirement, then elements within area are removed
 - If tow dimension is greater than 50% of tow length/width requirement, then elements within area are added until minimum dimension requirement is satisfied and the gaps are filled

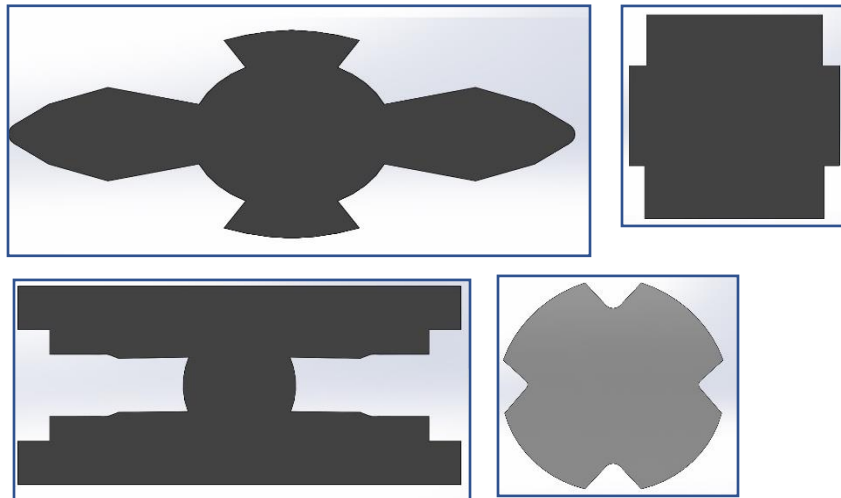


Figure 10: Edited ply shapes

Step 4: Converting to solids and making engineering drawing for full-scale print out.

SOLIDWORKS part drawing was generated and the paper size was set to real proportions.

For printout UTA racing plotter was used to take 20" x 10" print out as fixed in the print command of SOLIDWORKS.

STEP 5: NESTING process

This process helped to estimate the amount of material required and saved the material loss to make ply cutting efficient especially for which proved to be efficient

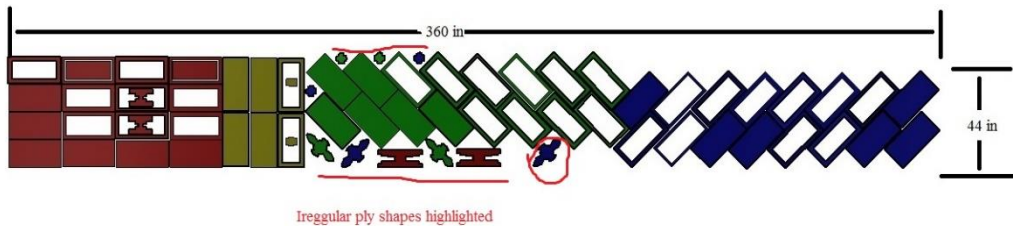


Figure 11: Ply arrangement for cutting through nesting process

3.5 Manufacturing

The effective layup of such kind of complex laminate Traditional hand layup was done using prepreg and laminate was cured in an autoclave. For manufacturing, the stacking sequence was decided by results obtained by shuffling optimization results and the ply shapes were taken from edited cad model after optimization process.

Material: Hexcel IM6/3506-1

Tooling: aluminum plate of 12" x 40" x 0.125" with vacuum valve

Cleaning agent: – Zyvax surface cleaner – Un1263

Sealant: Zyvax Sealer- Un1866

Release agent: Zyvax Multishield – Un1865

3.6.1 PLY CUTTING

The best way of cutting this type of ply shapes is to feed .dxf file to the ply cutting machine, but due to lack of resources manual ply cutting was done. To cut different irregular shapes paper templates were printed to true scale. As discussed in section 3.5.

Plies with 0° & 90° orientation were cut, keeping the wrap direction as 0° and fill direction as 90°, however, +/- 45° were cut by referencing a protector at +45° angles concerning table and the plies were cut different shape as shown in figure 12:

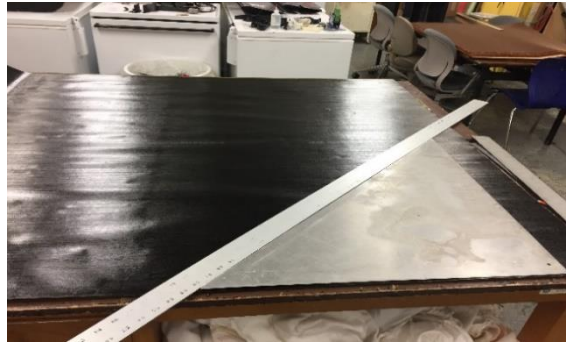


Figure 12: ply cutting at for 45° ply orientation

To lay up the irregular ply shapes, paper templates were used to locate the in- plane position of plies as shown below. There was a small misalignment of the full ply and bearing plies for orientation this might contribute to manufacturing defects.

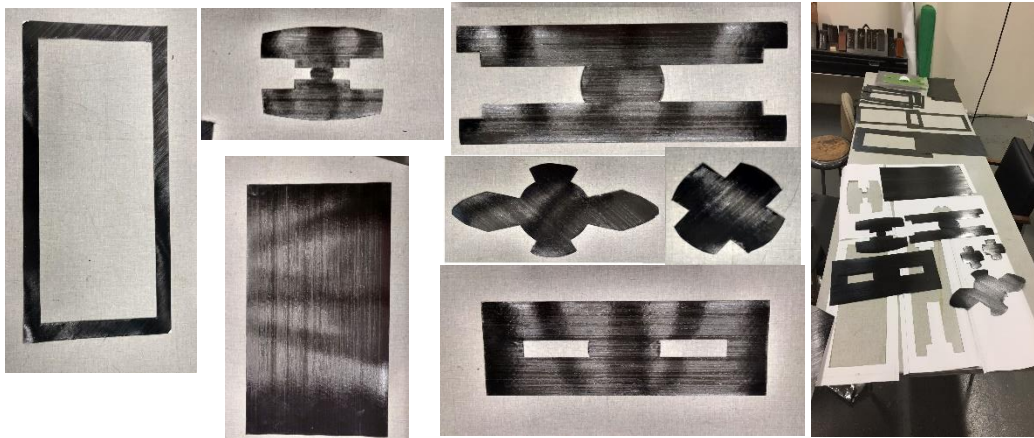


Figure 13: Ply shapes of Carbon fiber tape

The tool was cleaned with cleaning agent Zyvax surface cleaner – Un1263. After allowing to dry for 15 min another clear coat of Zyvax Sealer- Un1866 was applied to seal away any minor defects present on the tool surface. After 30 min of drying the sealant

coating, a final coat of Release agent Zyx Multishield – Un1865 was done on a tool for Assuring a smooth release of parts.

3.6.3 LAYUP

For accurate layup, two corners were matched with the previously laid ply to maintain fiber orientation consistently. This technique is timing consuming and requires lots practice for high accuracy layup. A rectangular fixture would have contributed more towards the precision of the layup.

Plies of 0 and 90 orientations were easy to a layup, +/- 45 orientation plies, especially the bearing plies were tight, and even a slight change in orientation would create an unbalanced. As the laminate was thick, Debulking process was done after layup of every ten plies to minimize possible amount voids.

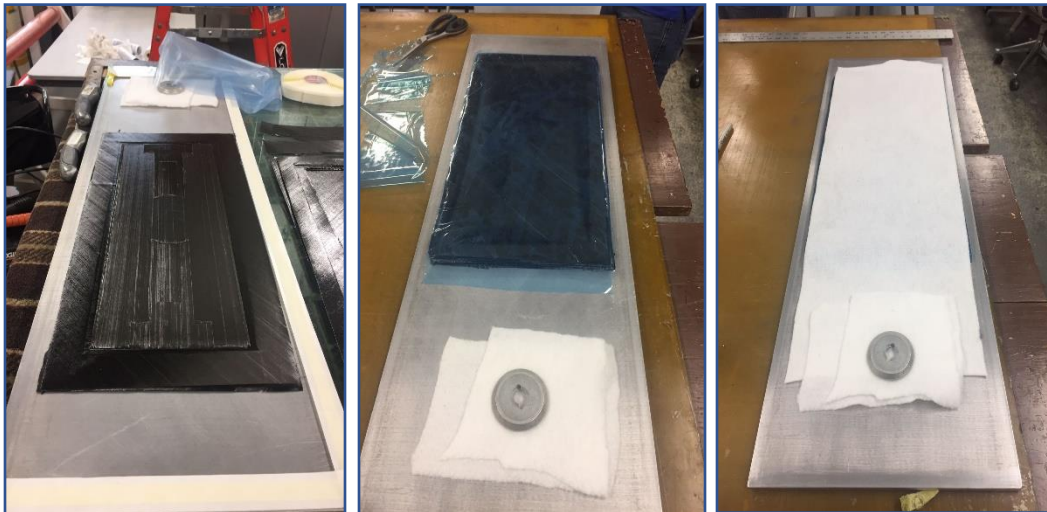


Figure 14: Lay-up process, release film, and breather

3.6.4 VACCUM BAGGING

After layup was complete, a non-perforated release film was placed on the top of laminate followed by breather or bleeder to allow escape excess of air and absorb excess

resin. The edges were covered with high-temperature tape to avoid any uneven flow through edges as the laminate were thick.



Figure 15: Vacuum bagging

3.6.5 AUTOCLAVE CURE CYCLE

Curing process was done in an autoclave. The cycle was programmed as per datasheet of Hexcel 3506-1 resin system as follows

1. Apply full vacuum and 85 psig pressure.
2. Heat at 3–5°F (1.8–3°C)/minute to 240°F (116°C).
3. Hold at 240°F (116°C) for 60–70 minutes.
4. Raise pressure to 100 psi; vent vacuum.
5. Raise temperature to 350°F (177°C) at 3–5°F (1.8–3°C)/minute.
6. Hold at 350°F (177°C) for 120 ± 10 minutes.
7. Cool at 2–5°F (1.2–3°C) to 100°F (38°C) and vent pressure.

Cure Cycle

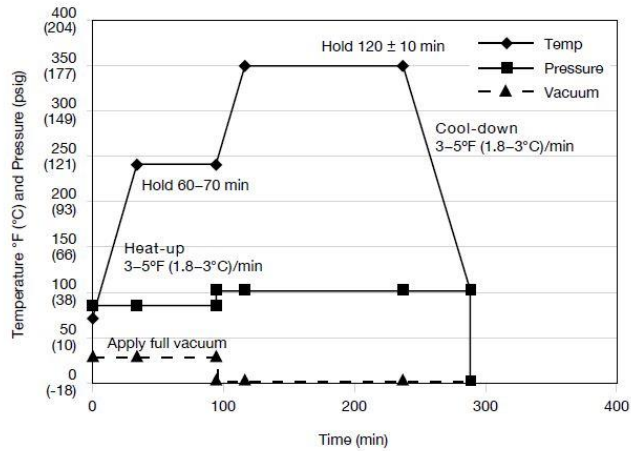


Figure 16: Demo cure cycle of HEXCEL IM6/3506-1.

3.7 Manufacturing induced defects

Manufactured laminate is as shown in figure 13, warpage of with small magnitude was observed in laminate at the transition of bearing plies to pad region and hence further study was carried as described in chapter 4 to predict behavior and magnitude of warpage. It is hard to measure the magnitude of warpage due to unavailability of resources, but the behavior was recorded by observing the laminate.

The laminate was warped in upward along the transition region as marked in red in figure X shown below

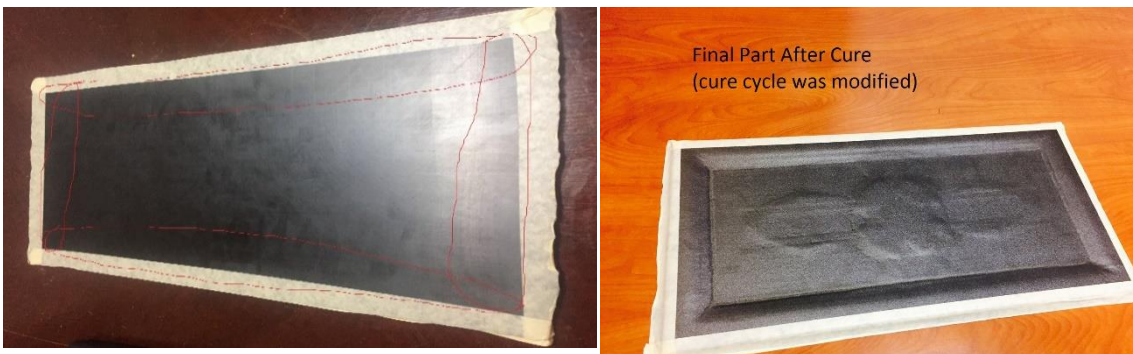


Figure 17: Cured laminate with warpage

CHAPTER 4: Warpage Prediction Model

The focus of this section establishes a relationship between Fiber orientation, ply-drops, and warpage effect due to this variation. The design of Experiments method was followed to predict behavior and magnitude of warpage. An analytical model, FEM and Experimental Model different number of ply drop for [0/45/90] family were developed to compare results for thermal loading on the laminate during cooling process of cure cycle. With the results of the analytical model for predicting warpage, it could be used to eliminate the defect in optimization process of the composite laminate in the design phase.

4.1 Analytical Model for predicting Warpage due to cooling cycle in cure process

The analytical model focuses mainly on calculating out of plane deformation due to thermal stress induced during cure cycle at the ply-drop intersection. The model can also handle asymmetric and unbalanced layup on the side of ply-drop (Zone 1 & 2) as shown figure 18(a) to give results regarding displacement in Z-direction.

Following FBD explains the effect of thermal forces and moment associated to it

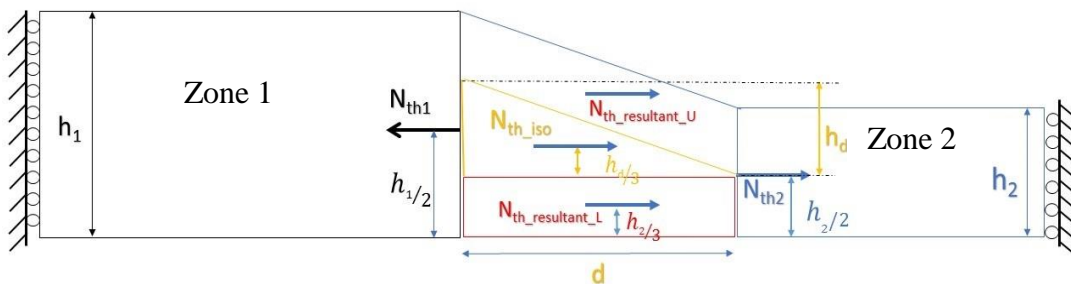


Figure 18(a): Actual ply-drop intersection FBD

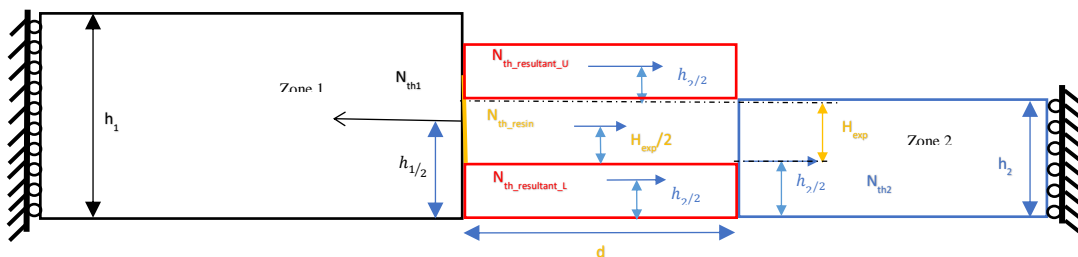


Figure 18(b): Modified ply-drop intersection FBD

Zone 1 is thick laminate, and zone 2 is thin laminate, the triangle in figure X(a) represents the resin pocket with height H_d . Where $H_d = t_{ply} * \text{number of plies dropped}$ & t_{ply} is post-cured ply thickness of a single lamina. h_1 & h_2 height, N_{th1} & N_{th2} are the thermal forces due to the CTE of laminate for zone 1 and zone 2 respectively.

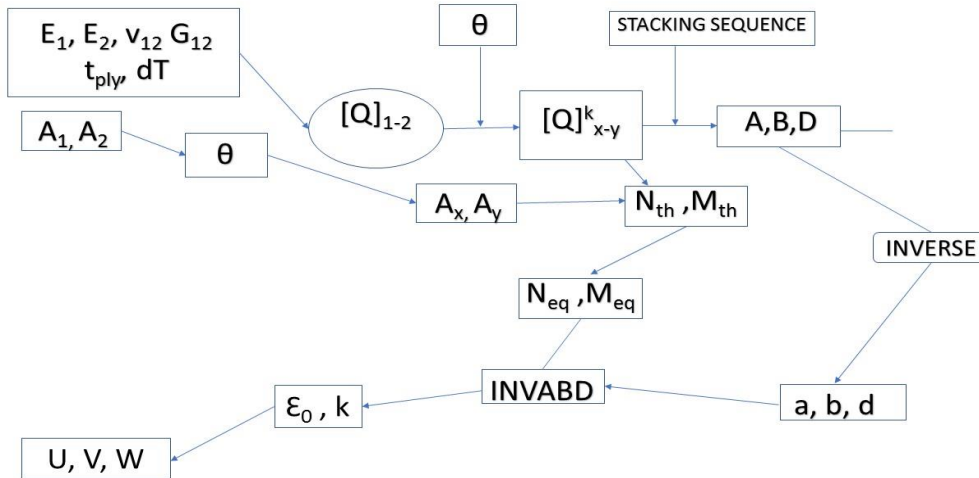


Figure 19: schematic of analytical model

Shown above is a schematic diagram of the procedure followed to explain the analytical model to calculate displacement in X, Y & Z direction. As of now, we are plotting displacement in Z-direction, but the same could be used to calculate X-Y displacement.

Material properties like Young's modulus, Poisson's ratio, modulus of rigidity, post-cure ply thickness and the temperature difference in cure cycle in local direction as the table shown below

Material properties	Values
E1	22000000 psi
E2	1300000 psi
V12	0.3

G ₁₂	2783700 psi
t _{ply}	0.0074
α ₁	-5 x 10 ⁻⁷ in/ F in
α ₂	1.5 x 10 ⁻⁵ in/ F in
Dt	-280 F

Table 5: Material properties of IM6/3506-1 for analytical model³.

- To find the local compliance matrix by the following equation

$$\begin{aligned}
 1. \quad s_{11} &= \frac{1}{E_1} & 2. \quad s_{22} &= \frac{1}{E_2} & 3. \quad s_{12} &= \frac{-\nu_{21}}{E_2} & 4. \quad s_{66} &= \frac{1}{G_{12}} \\
 \mathbf{S} &= \begin{bmatrix} s_{11} & s_{12} & 0 \\ s_{21} & s_{22} & 0 \\ 0 & 0 & s_{66} \end{bmatrix} \dots\dots\dots (a)
 \end{aligned}$$

$$[\mathbf{Q}]_{1-2} = [\mathbf{S}]^{-1} \dots\dots\dots (b)$$

- Furthermore, to convert the local matrix to global matrix the transformation matrix is applied

$$\mathbf{T}_\sigma = \begin{bmatrix} m^2 & n^2 & 2 * m * n \\ n^2 & m^2 & -2 * m * n \\ -m * n & m * n & m^2 - n^2 \end{bmatrix} \dots\dots\dots (c)$$

$$\mathbf{T}_\epsilon = \begin{bmatrix} m^2 & n^2 & 2 * m * n \\ n^2 & m^2 & -2 * m * n \\ -m * n & m * n & m^2 - n^2 \end{bmatrix} \dots\dots\dots (d)$$

where m=sin θ and n= cos θ (θ-> orientation of plies)

- Global Stiffness Matrix is as followed:

$$[\mathbf{Q}]_{x-y} = [\mathbf{T}_\sigma]^{-1} * [\mathbf{Q}]_{1-2} * [\mathbf{T}_\epsilon]^{-1} \dots\dots\dots (e)$$

with this global stiffness matrix has been used to calculate ABD matrix of the ply drop intersection with some modifications based on CLT⁴

$$[\mathbf{A}] = \sum_{k=1}^n [\mathbf{Q}]_{x-y} * t_k \dots\dots\dots (f)$$

$$[\mathbf{B}] = \sum_{k=1}^n [\mathbf{Q}]_{x-y} * t_k * (h_k + H_{exp}) \dots\dots\dots (g)$$

$$[D] = \sum_{k=1}^n [Q]_{x-y} (t_k * (h_k + H_{exp})^2 + \frac{t_k^3}{12}) \dots \dots \dots (h)$$

Where $H_{exp} = \frac{h_d}{6} + \frac{h_2}{2}$ & t_k is the ply thickness of kth layer & h_k is the height kth layer from bottom.

- Thermal forces and moments calculated⁴ as

$$N_{th} = \sum_{k=1}^n \{ [Q]_{x-y} * [\alpha]_{x-y} * (h_{k+1} - h_k) \} * \Delta T$$

$$M_{th} = \sum_{k=1}^n \{ [Q]_{x-y} * [\alpha]_{x-y} * (h_{k+1}^2 - h_k^2) \} * (\frac{\Delta T}{2})$$

ply-drop intersection has the plies on the upper and lower part of resin pocket.

Hence, the thermal load gets induced due to the both zone 1 and zone 2 as shown in

FBD and is assumed to be as

$$N_{th_resultant_U} = N_{th_resultant_L} = \frac{N_{th1} \cdot N_{th2}}{2}$$

But the overall force on the intersection of ply-drop is

$$N_{eq} = N_{th_resultant_U} + N_{th_resultant_L} + N_{th_resin}$$

Moment generated due this unbalanced thermal force is

$$M_{eq} = N_{th_resultant_U} * (H_{exp} + \frac{h_2}{2} + \frac{h_2}{2}) + N_{th_resultant_L} * \frac{h_2}{2} + N_{th_resin} * (\frac{H_{exp}}{2} + \frac{h_2}{2})$$

$$(N_{th_resin} \sim 0)$$

- The strain and curvatures are calculated as

$$\begin{bmatrix} \epsilon \\ \kappa \end{bmatrix} = \begin{bmatrix} A & B \\ B & D \end{bmatrix}^{-1} \begin{bmatrix} N_{eq} \\ M_{eq} \end{bmatrix}$$

- By classical lamination plate theory deformations U, V and W in X,Y and Z direction respectively is

$$U = \epsilon * x + \frac{1}{2} * \epsilon * y$$

$$V = \varepsilon * y + \frac{1}{2} * \varepsilon * x$$

$$W = -\frac{1}{2} (k * x^2 + k * x^2 + k * x * y)$$

where x and y are the matrices by which geometric dimension could be defined in the x-y plane. Please refer Appendix for MATLAB code.

4.2 Experimental model - Fabricating coupons

Experimental model is set of coupons with a different combination of orientation and number of ply drop as in table X. The coupons predict the behavior of the post cured laminate and if possible try to measure the flatness of the coupons to measure magnitude to get actual experimental data to set a baseline of comparison with the analytical model and FEM.

Coupons were made 1" X 4" with ply-drop of 1, 2, 3, 4, 8, 12, 16, 24 with stacking sequence with 0, +/- 45, 90 families with gradual ply-drops for some ply-drops from 1-6 and sudden ply-drops from 1-20 as mentioned in the table below:

Orientation	No. of Ply-drops								
0	1	2	3	4	5	6	8	12	16
-/+ 45	1	2	3	4	5	6	8	12	16
90	1	2	3	4	5	6	8	12	16

Table 6: Experimental model for different combination ply-drop and orientation

Procedure for making coupons was same as mentioned in section 3.6 except the 3.6.3. Layup for each coupon is done as a set of all 0 for each coupon with two cover plies at the top and two cover plies at the bottom. The similar layup was followed for 90, but in the case of +/-45, a balance was to be maintained to avoid any unbalanced forces as the aim was to record. The deformation due to ply drops for each -45 angled ply there was 45

angled ply for some ply drops with the top and bottom cover comprising a pair of $-/+45$ plies.

For example, stacking sequence for 4 ply drop layup for 0 and 90 was done as $[0\ 0\ 0\ 0\ 0\ 0\ 0\ 0]$ and $[90\ 90\ 90\ 90\ 90\ 90\ 90\ 90]$ respectively but for $-/+45$ it was $[-45\ 45\ -45\ 45\ 45\ -45\ 45\ -45]$. This was done to layup a balanced and symmetric laminate.

Curing of all coupons was done all in a single cure and only tool with same procedure just one time to avoid any variation due to obvious errors of autoclave process. Hence the results were easily comparable.

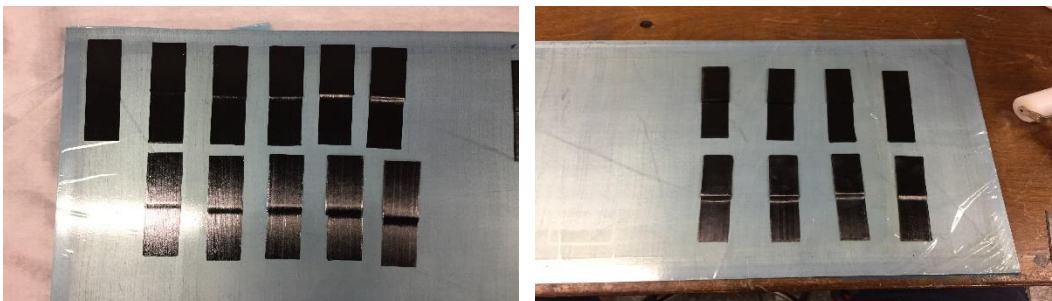


Figure 20 (a): Coupons before cure



Figure 20 (b): Coupons after cure

After curing it was observed that the factors causing warpage were majorly due to free expansion. Hence, another set of coupons were made with new layup technique to replicate the real senior as that in the composite laminate by restricting edges. To pick up the warpage caused due to the moment generated by ply-drop as explained in section 4.1. Therefore to restrict the edges for avoiding warpage effect due to free expansion, setup, as shown in the figure, was followed.

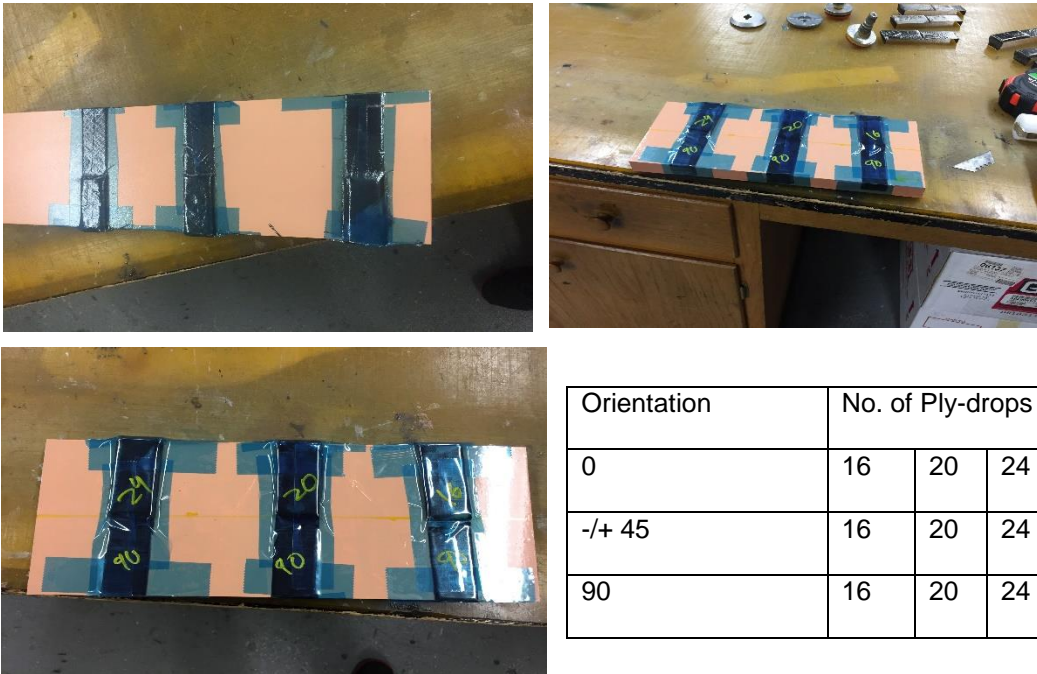


Figure 21: Coupons with restricted edges.

Orientation	No. of Ply-drops		
	16	20	24
0	16	20	24
-/+ 45	16	20	24
90	16	20	24

Table 7: Experimental model for different combination ply-drop and orientation with restricted edges

4.3 FEM model for predicting Warpage due to cooling cycle in cure process

Varying mesh size throughout overall coupon creates with 3D elements to pick up the displacement due to the ply-drop intersection in Z-direction (out-of-plane displacement). Following is the setup of FEM model to predict the out-of-plane warpage.

Geometry and types of coupons

Coupons were of dimension 4" x 1". The model has Hexa type 3D elements with a thickness of 0.0074". The mesh was refined at the ply-drop intersection to converge displacements at the intersection. A set of Hex elements were separately defined in the gap of ply drop intersection to as to replicate the real time model of resin pocket.

Orientation	No. of Ply-drops					
0	4	8	12	16	20	24
-/+ 45	4	8	12	16	20	24
90	4	8	12	16	20	24

Table 8: FEM model for different combination ply-drop and orientation

Material

Material properties used for plies was IM6/3506-1 carbon fiber prepreg from HEXCEL. In HyperMesh, the only anisotropic material card could refer to 3D elements, but there is a special case card as MAT9ORT, which takes orthographic material properties as input and calculates the remaining material constant and further used in simulations.

Following are the inputs required for MAT9ORT:

Material properties	Values
E ₁	22000000 psi
E ₂	1300000 psi
E ₃	1300000 psi
V ₁₂	0.3
V ₂₁ = V ₂₃	0.35
*G ₁₂	2783700 psi

*G ₂₃	321090 psi
*G ₃₁	2997900 psi
α ₁	-5 x 10 ⁻⁷ in/ F in
α ₂	1.5 x 10 ⁻⁵ in/ F in
Tref (the material temperature)	350 F

* Manually calculated values refer Appendix for MATLAB program and explanation

Table 9: Material properties for IM6/3506-1 prepreg

For the assigning material properties to the resin, MAT1 was used as it takes isotropic material properties as mentioned in the following table:

Material properties	Values
E	1300000 psi
V	0.35
G	750000 psi
A	1.5 x 10 ⁻⁵ in/ F in
Tref (the material temperature)	350 F

Table 10: Material properties for 3506-1

Property

In HyperMesh the type of elements is assigned its physical parameters like type of element, coordinate system, material, etc., all through properties. In this model, PSOLID property is used for both plies and resin.

Loads

Thermal load with a temperature gradient of -280 F was created to replicate the cooling process of cure cycle. This load was created on to every node of the coupon. The temperature distribution was assumed to be even, and the analysis was considered as a time-independent form of simulation.

Boundary conditions

Constraining model in the right position and by the correct degree of freedom was crucial to picking displacement in the Z direction (along thickness). The aim was to get overall Z displacement of entire coupon due to ply-drop under thermal loading on the free expansion of Coupons. As the magnitude was of the load was low it was necessary to concentrate effect of the thermal load at the ply-drop intersection. This achieved by constraining model at the end by restricting displacement in X, Y and rotation in all three degrees of freedom so only 1 DOF as shown in figures below

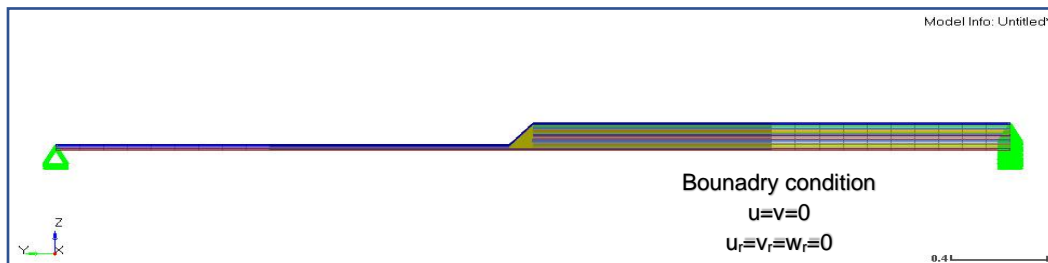


Figure 22: Roller support at the end

Material Coordinate System for 3D elements

In HyperMesh 3D elements could not be given material orientation directly as it is possible with 2D. A local coordinate system is defined. And after the local coordinate system was assigned to property, the material orientation of elements was defined as follows

Analysis-> System-> material Orientation-> select by system axis-> local axis 1.

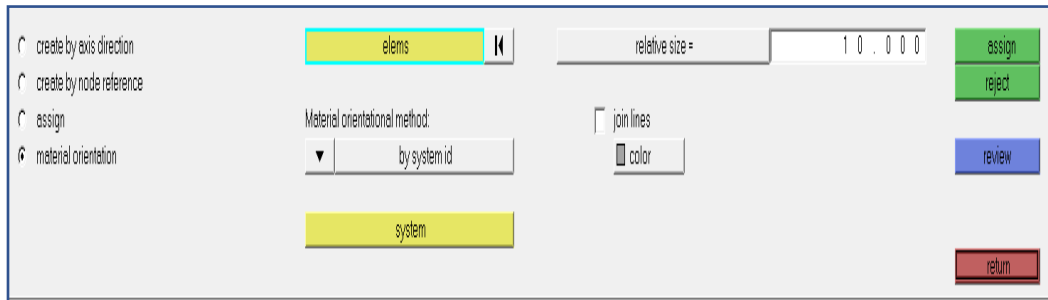


Figure 23: command in HyperMesh for material orientation for 3D elements

The model formation for the composite laminate for predicting warpage is same with same loading conditions and similar boundary condition of roller support. The only change is the geometry which is same as mentioned in 3.2.1. The property is the same PSOLID as used for coupons only different property is defined for various orientation as for each orientation a separate local axis has to be defined which can be only assigned to elements through the property.

Chapter 5: Results

5.1 Analytical model

The model calculates strain and curvature generated due to ply-drop intersection under thermal loading induced due to cooling cycle of the curing process of the laminate. The program mentioned in Appendix B-1 calculates results for a coupon of 4" x 1". These plots are from 1.9 to 2.1 as the aim of this analytical model is to study the behavior of laminate at the ply-drop intersection and help understand the magnitude and direction of warpage due to it. The model is general and can calculate form various orientation and ply-drop combinations, results discussed below are focused on the ply-drop intersection.

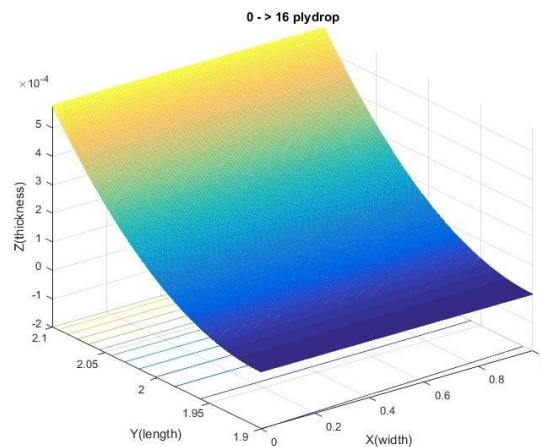


Figure 24: Deformation results based on the analytical model for 0 with 16

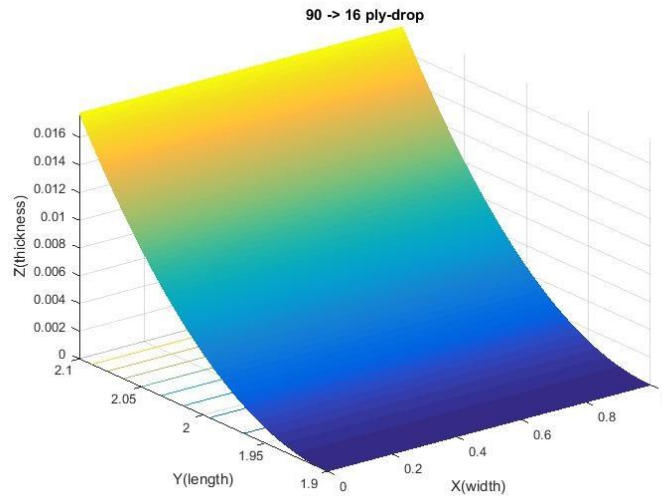


Figure 25: Deformation results based on the analytical model for 90 with 16 ply-drops

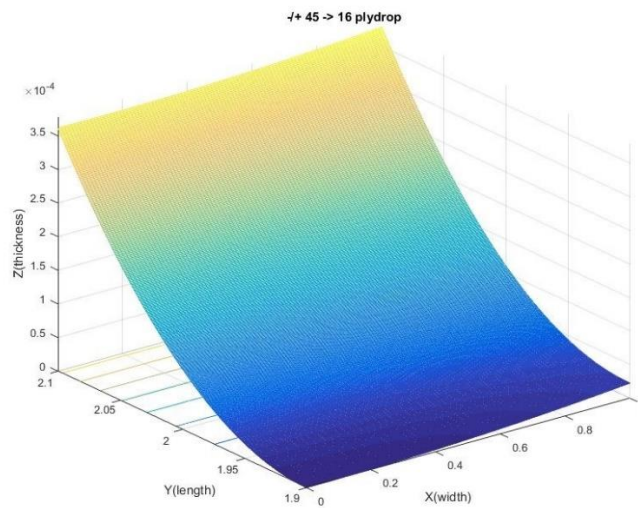


Figure 26: Deformation results based on the analytical model for -/+45 with 16 ply-drops

The above plot in figure 19, figure 20, and figure 21 is for 0, -/+45, and 90 orientations respectively. The plot is X vs. Y vs. Z representing width, length, and thickness of coupons. Out of plane deformation in positive Z-direction with 16 ply-drops from 2 to 2.1 on the y-

axis in figure 21. The small magnitude of warpage incrementing with length from the ply-drop junction was observed and the direction was in positive Z-direction. In case, of +/- 45 apart from the warpage along the length there was also twisting observed in the direction of fiber orientation.

Results were obtained several model, and the angle of warpage was calculated as shown below:

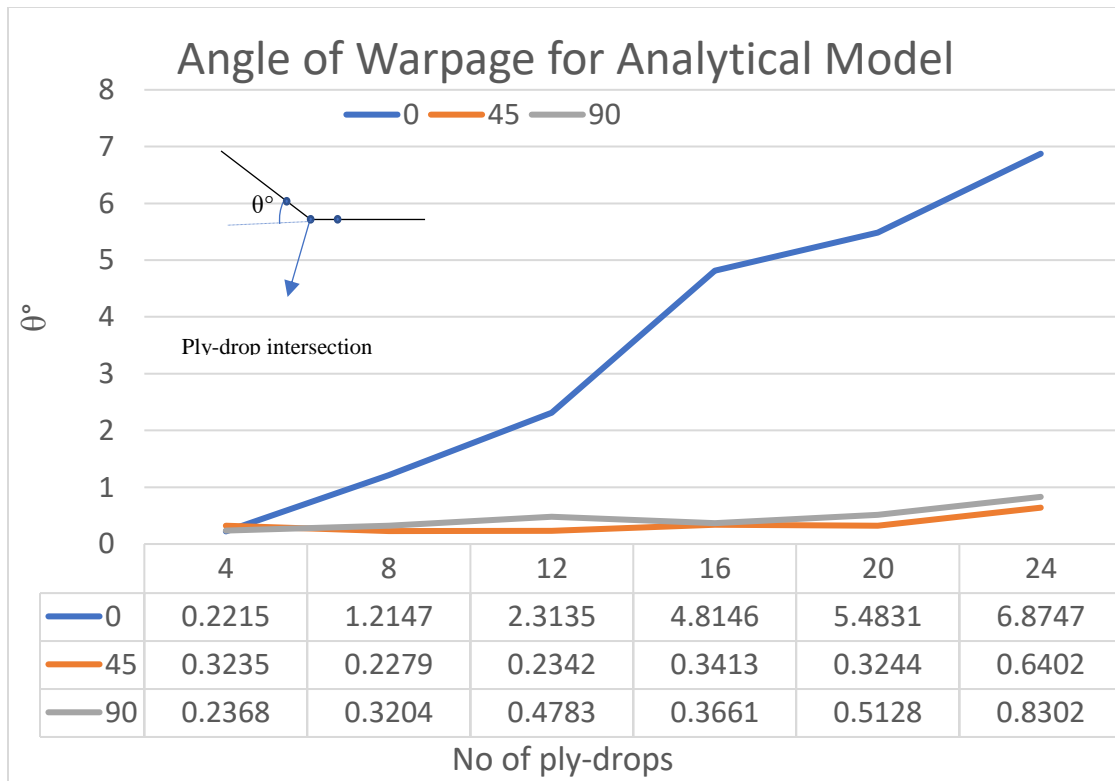


Figure 27: Trends of change in angle of with ply-drops and the orientation for Analytical model

5.2 Experimental model

The experimental design comprised of a number of different combinations of layups as mentioned in section 4.2. Out of which up to 16 ply-drop in all three combinations of orientation. Due to unavailability of resources the magnitude of this warpage was not

possible as the warpage was in order ranging from 10^{-3} to 10^{-4} of an inch and below. There was visually noticeable warpage detected for ± 45 orientation the similar behavior as predicted by the analytical model was observed. Hence more coupons with higher ply-drops are needed to be fabricated for all three-different orientation. Going beyond 16 ply-drop at a time would violate the actual design scenario. Below are the images of coupons manufactured with 16 ply-drop in figure X and figure X has images for the coupons fabricated below 16 ply-drop.

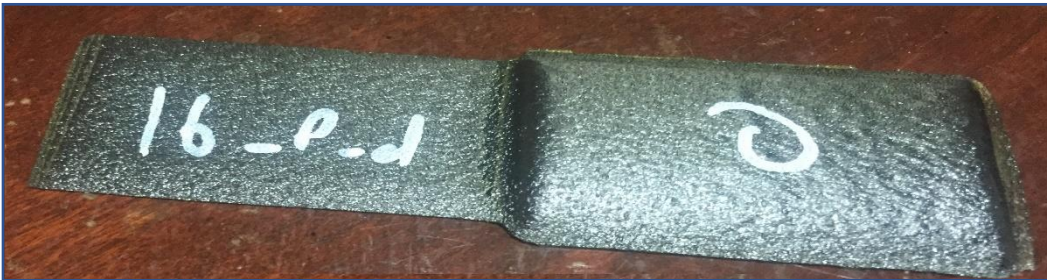


Figure 28: 0 orientation Layup with 16 ply-drop



Figure 29: ± 45 orientation Layup with 16 ply-drop



Figure 30: 90 orientation Layup with 16 ply-drop

With the new set of coupons with restricted edges showed similar result as that of the coupons layed earlier. There was no measureable amount of warpage that could be observed. But there was a deformation in $\pm 45^\circ$ as due to the coupling effect due to the presence of D_{16} and D_{26} which collectively causes bending twisting effect, coupling effect.

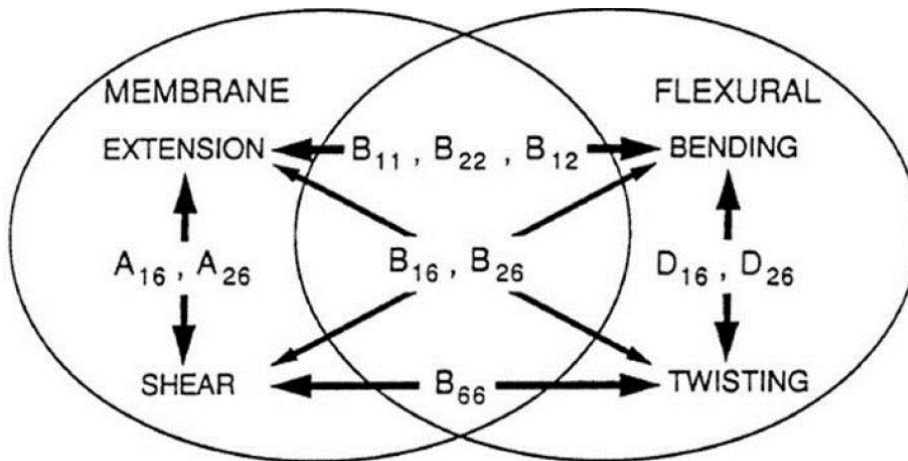


Figure 31: coupling effect for a classical lamination theory³⁴



Figure 32(a): Coupons with restricted edges after cure

The possible reasons for not obtaining warpage could be:

The pressure during cure cycle acts on vacuum bag which restricts the z-direction warpage. Out of plane deformation occurs due to the moment generated at plydrop intersection, the values could be obtained from analytical model as 25.3964 lbf-in for 0°, 6.7743 lbf-in for 90° and 9.5768 lbf-in for -/+ 45° which is less than counter moment generated at ply-drop intersection due to vacuum bag exerting pressure of 100 psi over the area of 2" x 1" on thin laminate. Assuming a point load of magnitude 50 lbf at midpoint of the area. This force creates a counter moment of 50 lbf-in. Hence, overriding the effect of moment generated by thermal force as shown in figure below:

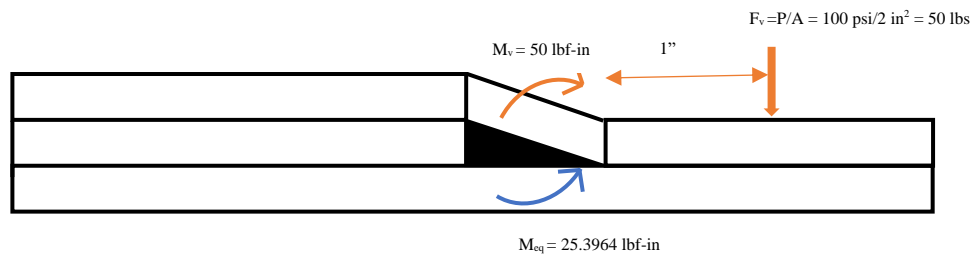


Figure 32 (b): Moment at ply-drop intersection

There is need of a layup technique by which the warpage due ply-drop effect could be amplified enough to measure and calibrate the analytical model in order to yield accurate results.

5.3 FEM model

Fem could predict the effect of ply-drop on the entire coupon. But the results were more focused on the behavior of the ply-drop intersection.

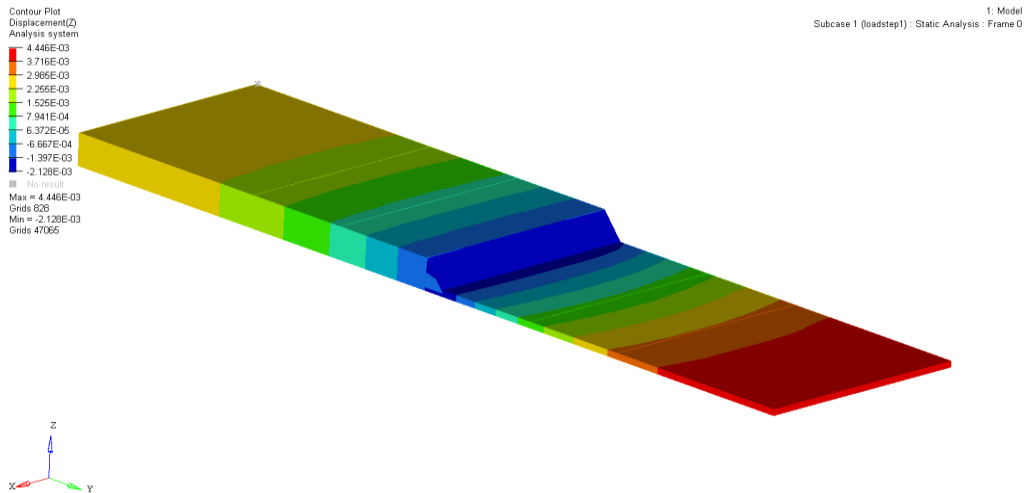


Figure 33(a): 0° plies with 16 ply-drops

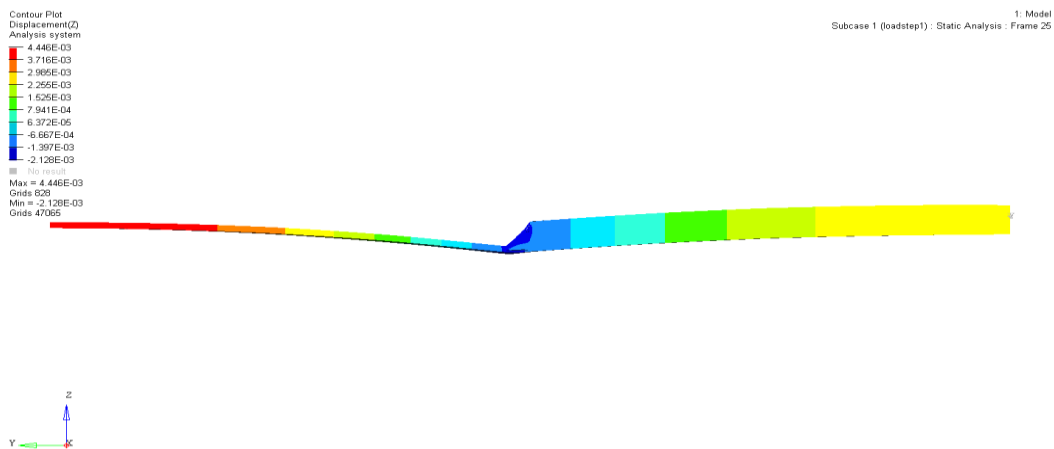


Figure 33(b): 0° plies with 16 ply-drops 100x exaggerated

Warpage could be observed in figure 33(a) and Figure 33(b) after results are exaggerated by 100x. Unequal displacement of the edges in Z-direction is possibly because of the laminate thickness difference. The thin laminate over left of ply-drop intersection is displaced more cause of less weight to resist compared to the thick laminate at right.

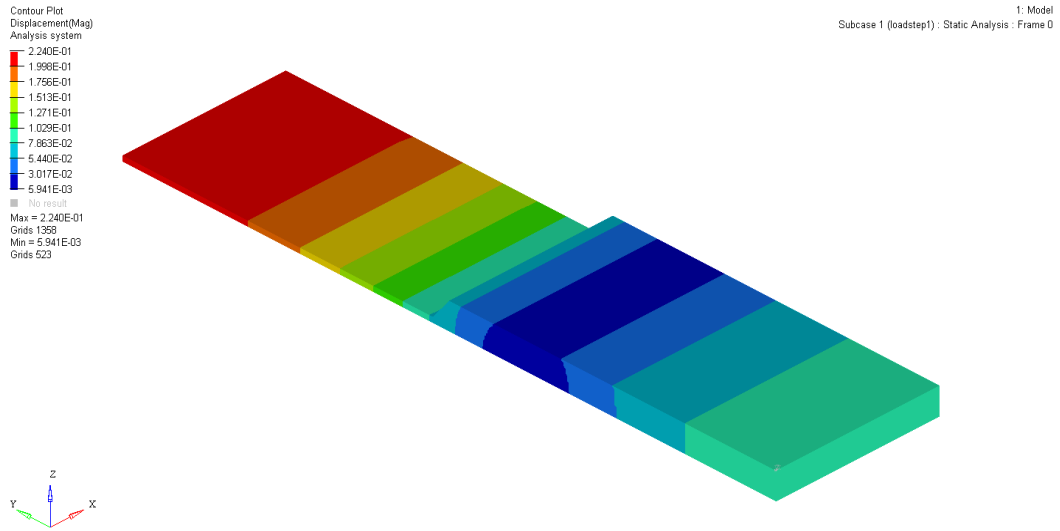


Figure 34(a): 90° plies with 16 ply-drops

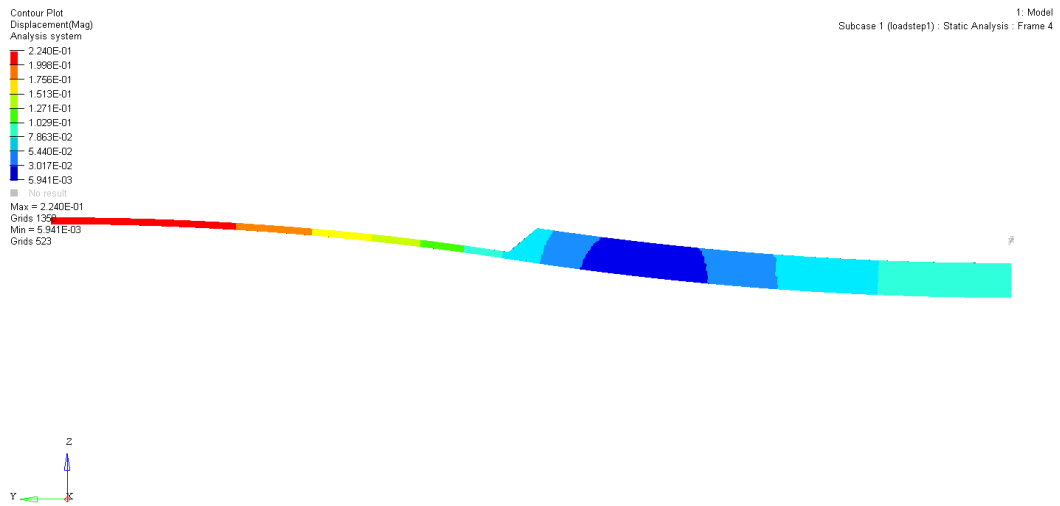


Figure 34(b): 90° plies with 16 ply-drops 100x exaggerated

Figure 34(a) and figure 34(b) results plots for 90° ply orientations and the magnitude is higher compared to 0 ply orientation, but the behavior is similar, that is there is an incremental change in length away from the ply-drop intersection in both direction.

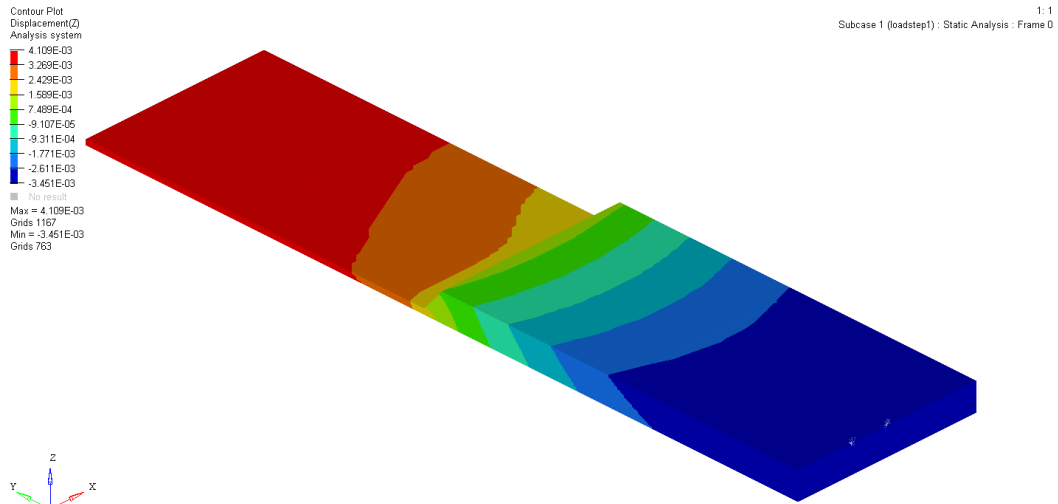


Figure 35(a): $\pm 45^\circ$ plies with 16 ply-drops

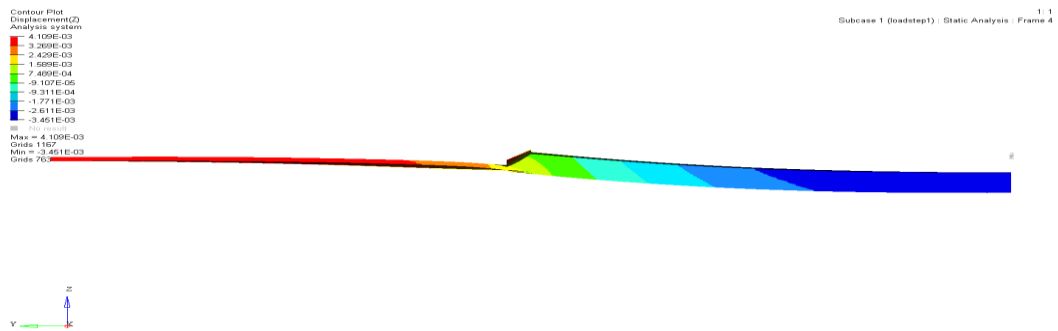


Figure 35(b): $\pm 45^\circ$ plies with 16 ply-drops 100x exaggerated

The results are shown in figure 35(a) and Figure 35(b) is for $\pm 45^\circ$ ply orientation. It is observed that warpage is a function of length and width and due to which twisting is the effect is induced.

Below is the trend which shows the change in angle at ply-drop intersection

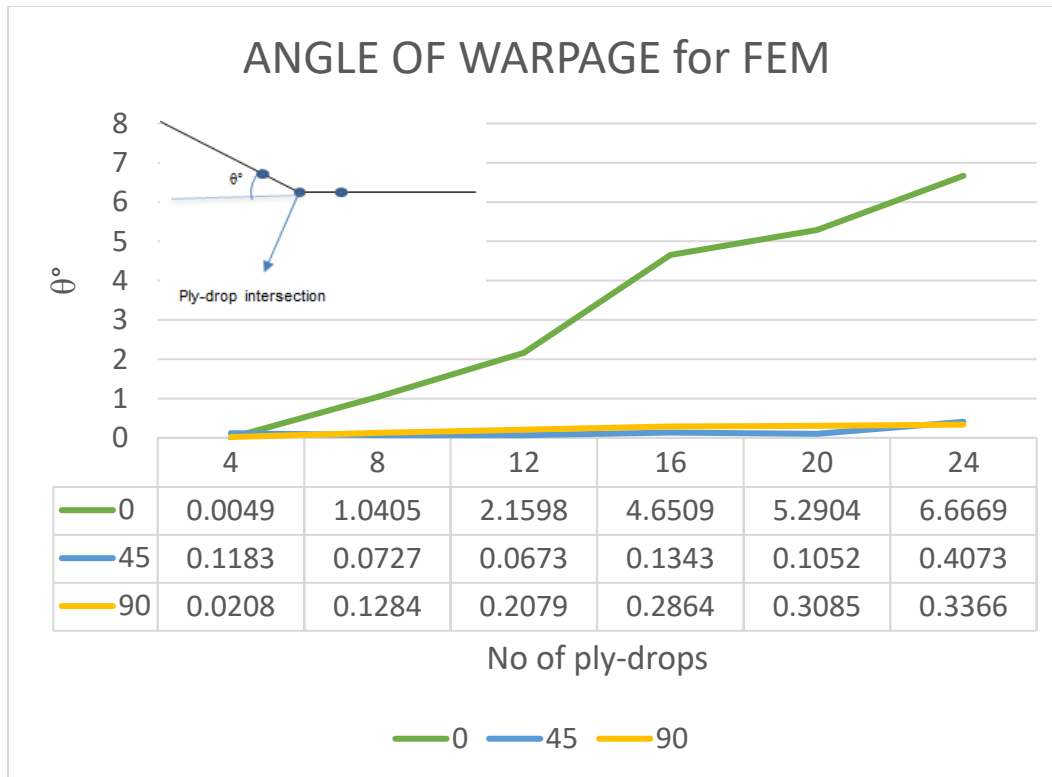


Figure 36: Trends of change in angle of with ply-drops and the orientation for FEM

angle of warpage increases the number of ply-drop increases.

Angle of warpage is quite low in magnitude. Sudden change in 0° compared to 90° and $\pm 45^\circ$ can be observed, reason for this is fiber in line transfers moment generated with less matrix resistance compared to 90° and $\pm 45^\circ$.

5.4 Comparison of results from all three models

For validation of analytical model and FEM, the results are compared as follows

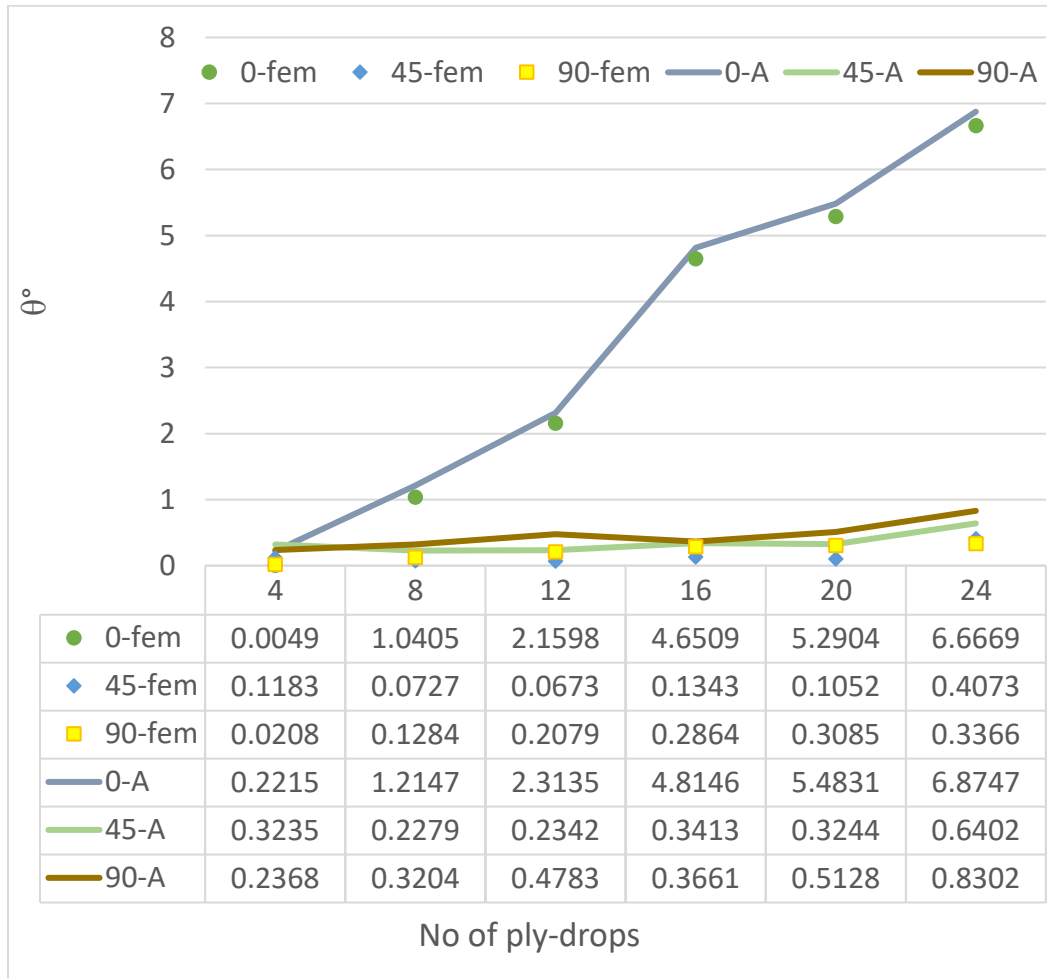


Figure 37: Comparison of FEM and Analytical results

This results are in close agreement, but in general the models are not reliable until the analytical model is calibrated with the responses from experimental model.

FEM with 3D elements generated of fabricated composite laminate.

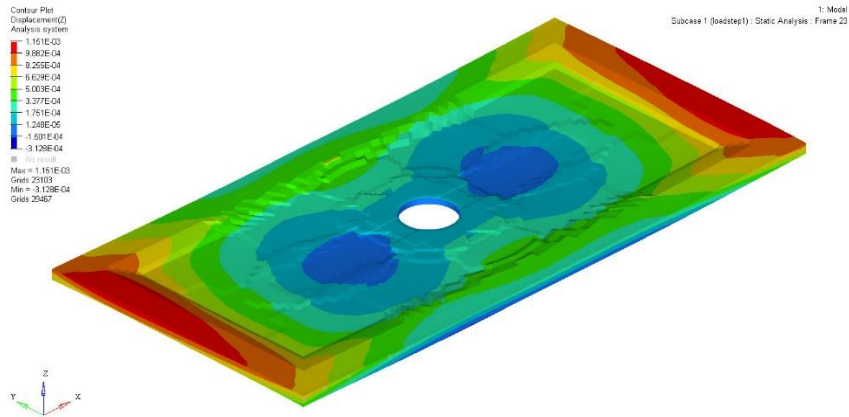


Figure 38: Z-displacement for composite laminate after thermal loading

It was observed that the maximum Z-displacement could be seen in the same location as that of in the actual laminate as shown in figure 17.

Chapter 6: Conclusion & Future work:

In three phase optimization process, several models were subjected to optimization process with a combination of different values of total ply slope and total ply drop in free-size and size optimization in the previous study¹.

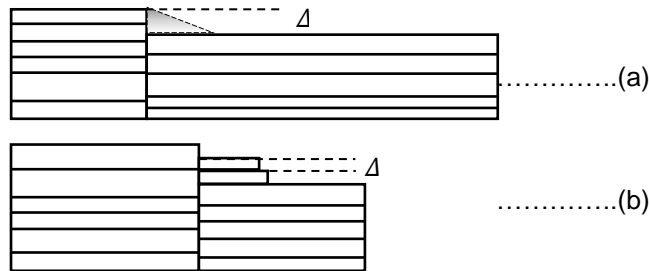


Figure 39: (a) Ply drop and slope effect on larger panel¹ (b) Ply drop effect on smaller panel¹

The value of total ply slope and total ply drop assigned in three-phase optimization process should have a minimum range of variation. To get manufacture-able stacking sequence

with minimum constraint violation. By manufacturing the complete laminate with variable ply-drops series of ply drops as shown in figure

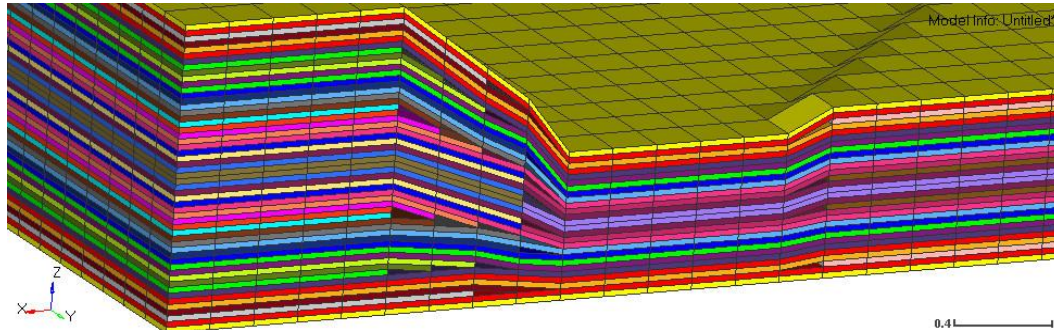


Figure 40: Cross-sectional view of optimize composite plate

The warpage due to ply-drops could be induced in thick laminates due to the manufacturing process because of the set of the moment generated by each ply-drop in the entire laminate.

Results from the Analytical model and FEM are in close agreement in warpage prediction due to ply-drops during the manufacturing process. The analytical model is computationally fast and suitable for integration into the automated optimization process to eliminate defects in the design phase after further refinement of the model based on the responses from DOE.

FUTURE WORK

1. Layup of coupons has to be done to increase the moment generated at ply-drop intersection which will be more than the counter moment generated due to vacuum bagging and cure cycle pressure to get a measurable warpage with different combinations of ply-drops and stacking sequence. Following are some suggestions for the same:
 - i. Increase the cover plies from four to eight
 - ii. Change the material which requires low pressure for cure.
2. After the measurable warpage, could be mapped from the experimental model, the height of the resin pocket H_{exp} mentioned in FBD figure 18(b) has to be calibrated to refine the analytical model.
3. Transient analysis could be performed, stiffness matrix and thermal load could be made time dependent.

4. Exact Temperature distribution can be found from thermal analysis and accordingly thermal load could be applied, or a combined structural and thermal analysis could be done to refine FEM and compare results with experimental model to validate results.
5. Detection of resin pockets through nondestructive testing and Analysis for prediction of knock down strength could be carried out.

APPENDIX A

FEM file structure for shuffling optimization

```

$$
$$ Optistruct Input Deck Generated by HyperMesh Version : 14.0.130.21
$$ Generated using HyperMesh-Optistruct Template Version : 14.0.130
$$
$$ Template: optistruct
$$
$$
$$ optistruct
$
RESPRINT=EQUA
OUTPUT,SZTOSH,YES
SCREEN OUT
CFAILURE(H3D,NDIV=1) = ALL
CSTRAIN(H3D,ALL,NDIV=1) = YES
CSTRESS(H3D,ALL,NDIV=1) = ALL
$-----$
$$ Case Control Cards $
$-----$
$$
$$ OBJECTIVES Data
$$
$
$HMNAME OBJECTIVES 1objective
$
DESOBJ(MIN)=15
$
$
$HMNAME LOADSTEP 1"Shear_Only" 1
$
SUBCASE 1
 LABEL Shear_Only
 SPC = 8
 LOAD = 2
 DESSUB = 15
$
$HMNAME LOADSTEP 2"buck_Shear_Only" 4
$

```

```

SUBCASE 2
  LABEL buck_Shear_Only
  SPC = 8
  METHOD(STRUCTURE) = 1
  STATSUB(BUCKLING) = 1
  DESSUB = 16
$ DESSUB = 17
$
$HMNAME LOADSTEP 3"Compression_Only" 1
$
SUBCASE 3
  LABEL Compression_Only
  SPC = 8
  LOAD = 3
  DESSUB = 17
$
$HMNAME LOADSTEP 4"buck_Compression_Only" 4
$
SUBCASE 4
  LABEL buck_Compression_Only
  SPC = 8
  METHOD(STRUCTURE) = 1
  STATSUB(BUCKLING) = 3
  DESSUB = 18
$ DESSUB = 19
$
$HMNAME LOADSTEP 5"Tension" 1
$
SUBCASE 5
  LABEL Tension
  SPC = 8
  LOAD = 4
  DESSUB = 19
$
$-----
$$ HYPERMESH TAGS
$-----
$$BEGIN TAGS
$$END TAGS
$
BEGIN BULK
$
$HMNAME PLYS 1"PLYS_1"
$HWCOLOR PLYS 1 4
PLY 1 2 0.005 -45.0 YES 0.005
+ 7
$
$HMNAME PLYS 2"PLYS_2"
$HWCOLOR PLYS 2 3
PLY 2 2 0.005 0.0 YES 0.005
+ 2

```

```

$
$HMNAME PLYS          3"PLYS_3"
$HWCOLOR PLYS          3  5
PLY  3  2  0.005 45.0 YES  0.005
+  11
$
$HMNAME PLYS          4"PLYS_4"
$HWCOLOR PLYS          4  6
PLY  4  2  0.005 90.0 YES  0.005
+  16
$
$HMNAME PLYS          5"PLYS_5"
$HWCOLOR PLYS          5  4
PLY  5  2  0.005 -45.0 YES  0.005
+  21
$
$HMNAME PLYS          6"PLYS_6"
$HWCOLOR PLYS          6  4
PLY  6  2  0.005 -45.0 YES  0.005
+  36
$
$HMNAME PLYS          7"PLYS_7"
$HWCOLOR PLYS          7  4
PLY  7  2  0.005 -45.0 YES  0.005
+  37
$
$HMNAME PLYS          8"PLYS_8"
$HWCOLOR PLYS          8  5
PLY  8  2  0.005 45.0 YES  0.005
+  38
$
$HMNAME PLYS          9"PLYS_9"
$HWCOLOR PLYS          9  4
PLY  9  2  0.005 -45.0 YES  0.005
+  38
$
$HMNAME PLYS          10"PLYS_10"
$HWCOLOR PLYS          10  5
PLY  10  2  0.005 45.0 YES  0.005
+  38
$
$HMNAME PLYS          11"PLYS_11"
$HWCOLOR PLYS          11  5
PLY  11  2  0.005 45.0 YES  0.005
+  22
$
$HMNAME PLYS          12"PLYS_12"
$HWCOLOR PLYS          12  24
PLY  12  2  0.005 45.0 YES  0.005
+  36

```



```

$
$HMNAME PLYS          13"PLYS_13"
$HWCOLOR PLYS          13  5
PLY 13  2  0.005 45.0 YES  0.005
+ 37
$
$HMNAME PLYS          14"PLYS_14"
$HWCOLOR PLYS          14  3
PLY 14  2  0.005 0.0  YES  0.005
+ 2
$
$HMNAME PLYS          15"PLYS_15"
$HWCOLOR PLYS          15  3
PLY 15  2  0.005 0.0  YES  0.005
+ 2
$
$HMNAME PLYS          16"PLYS_16"
$HWCOLOR PLYS          16  3
PLY 16  2  0.005 0.0  YES  0.005
+ 4
$
$HMNAME PLYS          17"PLYS_17"
$HWCOLOR PLYS          17  3
PLY 17  2  0.005 0.0  YES  0.005
+ 5
$
$HMNAME PLYS          18"PLYS_18"
$HWCOLOR PLYS          18  6
PLY 18  2  0.005 90.0 YES  0.005
+ 16
$
$HMNAME PLYS          19"PLYS_19"
$HWCOLOR PLYS          19  3
PLY 19  2  0.005 0.0  YES  0.005
+ 6
$
$HMNAME PLYS          20"PLYS_20"
$HWCOLOR PLYS          20  5
PLY 20  2  0.005 45.0 YES  0.005
+ 12
$
$HMNAME PLYS          21"PLYS_21"
$HWCOLOR PLYS          21  4
PLY 21  2  0.005 -45.0 YES  0.005
+ 8
$
$HMNAME PLYS          22"PLYS_22"
$HWCOLOR PLYS          22  5
PLY 22  2  0.005 45.0 YES  0.005
+ 11

```

```

$
$HMNAME PLYS          23"PLYS_23"
$HWCOLOR PLYS          23  5
PLY 23  2  0.005 45.0 YES  0.005
+ 11
$
$HMNAME PLYS          24"PLYS_24"
$HWCOLOR PLYS          24  4
PLY 24  2  0.005 -45.0 YES  0.005
+ 7
$
$HMNAME PLYS          25"PLYS_25"
$HWCOLOR PLYS          25  4
PLY 25  2  0.005 -45.0 YES  0.005
+ 7
$
$HMNAME PLYS          26"PLYS_26"
$HWCOLOR PLYS          26  5
PLY 26  2  0.005 45.0 YES  0.005
+ 15
$
$HMNAME PLYS          27"PLYS_27"
$HWCOLOR PLYS          27  4
PLY 27  2  0.005 -45.0 YES  0.005
+ 10
$
$HMNAME PLYS          28"PLYS_28"
$HWCOLOR PLYS          28  6
PLY 28  2  0.005 90.0 YES  0.005
+ 19
$
$HMNAME PLYS          29"PLYS_29"
$HWCOLOR PLYS          29  6
PLY 29  2  0.005 90.0 YES  0.005
+ 38
$
$HMNAME PLYS          30"PLYS_30"
$HWCOLOR PLYS          30  3
PLY 30  2  0.005 0.0 YES  0.005
+ 38
$
$HMNAME PLYS          31"PLYS_31"
$HWCOLOR PLYS          31  3
PLY 31  2  0.005 0.0 YES  0.005
+ 37
$
$HMNAME PLYS          32"PLYS_32"
$HWCOLOR PLYS          32  3
PLY 32  2  0.005 0.0 YES  0.005
+ 36

```

```

$
$HMNAME PLYS          33"PLYS_33"
$HWCOLOR PLYS        33  4
PLY 33  2  0.005 -45.0 YES  0.005
+ 38
$
$HMNAME PLYS          34"PLYS_34"
$HWCOLOR PLYS        34  3
PLY 34  2  0.005  0.0  YES  0.005
+ 20
$
$HMNAME PLYS          35"PLYS_35"
$HWCOLOR PLYS        35  3
PLY 35  2  0.005  0.0  YES  0.005
+ 38
$$
$$ Stacking Information for Ply-Based Composite Definition
$$
$
$HMNAME LAMINATES     3"LAM_3"
$HWCOLOR LAMINATES    3  3
STACK 3  SYM  4  1  7  10  21  24
+ 27  33  31  34  22  25  28  2
+ 3  12  15  11  16  14  13  9
+ 8  6  5  18  17  19  35  29
$
$HMNAME OPTICONTROLS  1"optistruct_opticontrol" 1
$
DOPTPRM DESMAX 1000  GBUCK 0
$
$HMNAME OPTITABLEENTRS  1"optistruct_tableentries" 14
$
DTABLE  F1xt  0.0  F1yt  0.0  F2xt 2000.0  F2yt  0.0
+  F1xc  0.0  F1yc  0.0  F2xc -2000.0  F2yc  0.0
+  F1xs 2000.0  F1ys  0.0  F2xs  0.0  F2ys 2000.0
+  Sym  2.0  diam  0.25 strnCmp 0.0042  BrgLim 80000.0

$HMNAME DESVARS      3DCOMP3.1
DSHUFFLE  3  STACK  3
+  MAXSUCC  ALL  4
+  COVER  1  -45.0  0.0  45.0  90.0
$HMNAME DESVARS      3DCOMP3.1.1
DSHUFFLE  3  STACK  3
+  MAXSUCC  ALL  4
+  COVER  1  -45.0  0.0  45.0  90.0
$$
$$ OPTIRESPONSES Data
$$
DRESP1 15  Mass  MASS
DRESP1 69  BucklingLAMA 1

```

```

DRESP1 78   MaxStrn CSTRAIN PCOMP      SMAP  ALL  3
$$
$$ OPTICONSTRAINTS Data
$$
$
$HMNAME OPTICONSTRAINTS   9MaxStrn
$
DCONSTR   9   78-0.003 0.003
$
$HMNAME OPTICONSTRAINTS  10MinStrn
$
DCONSTR  10   79-0.003 0.003
$
$HMNAME OPTICONSTRAINTS  11CFailure
$
DCONSTR  11   80   1.0
$
$HMNAME OPTICONSTRAINTS  14BUCKLING
$
DCONSTR  14   691.02

DCONADD  15   9   10  11

DCONADD  16  14

DCONADD  17   9   10  11

DCONADD  18  14

DCONADD  19   9   10  11

$HMNAME SYSTCOL   1 "auto1"
$HWCOLOR SYSTCOL   1   3
$$
$$ SYSTEM Data
$$
CORD3R   1  3101  7134  6011
$
$HMMOVE   2
$   1THRU   8500
$$
$$-----$
$$ HyperMesh name and color information for generic components      $
$$-----$
$HMNAME COMP           2"Middle Surface"   3 "CarbonTape" 4
$HWCOLOR COMP           2   52
$
$HMNAME COMP           3"component1"
$HWCOLOR COMP           3   4

```

```

$
$HMNAME COMP          4"component2"
$HWCOLOR COMP        4   5
$
$HMNAME COMP          5"component3"
$HWCOLOR COMP        5   6
$

$

$
$HMNAME PROP          3"CarbonTape" 4
$HWCOLOR PROP        3   7
PCOMPP    3 BOTTOM    18000.0  STRN
$$
$$ MAT8 Data
$$
$HMNAME MAT           2"CarbonEpoxy" "MAT8"
$HWCOLOR MAT         2   7
MAT8    22.2+7 1300000.0.3  750000.0  516000.00.056
+  0.5  0.4  70.0  170000.0170000.06500.0  28000.0 10000.0
$$
$$$$-----$$
$$ HyperMesh Commands for loadcollectors name and color information $
$$$$-----$$
$HMNAME LOADCOL      5"Compression"
$HWCOLOR LOADCOL    5   5
$$
$HMNAME LOADCOL      6"Tension"
$HWCOLOR LOADCOL    6   5
$$
$HMNAME LOADCOL      7"Shear"
$HWCOLOR LOADCOL    7   5
$$
$HMNAME LOADCOL      8"Constraints"
$HWCOLOR LOADCOL    8   5
$$
$$ EIGRL cards
$$
$HMNAME LOADCOL      1"EIGRL"
$HWCOLOR LOADCOL    1   7
EIGRL    1  0.0      2          MAX
ENDDATA
$$
$$$$-----$$
$$   Data Definition for AutoDV          $$
$$$$-----$$
$$
$$$$-----$$
$$   Design Variables Card for Control Perturbations    $$

```

```

$$$$-----$$
$$$$
$$$$-----$
$$$ Domain Element Definitions $
$$$$-----$
$$$$
$$$$-----$$
$$$ Control Perturbation $$$
$$$$-----$$$

```

APPENDIX B MATLAB code

B-1 Analytical model

```

%% By Sitanshu Pandya
clear all; close all
%% Material properties
E1=22000000;
E2=1300000;
G12=2783700;
v12=0.3;
Alpha_12=[-5e-7;1.5e-5;0];
dT=280; %F
tply=0.0074;
%% S matrix
S11=1/E1;
S12=-v12/E1;
S22=1/E2;
S66=1/G12;
S=[S11 S12 0; S12 S22 0; 0 0 S66];
%% Q matrix
Q=inv(S);
%% Stacking Sequence for ZONES
% zone1=[90 90 90 90 90 90 90 90 90 90 90 90 90 90 90 90
90 90];
% zone2=[90 90 90 90];
zone1=[0 0 0 0 0 0 0 0 0 0 0 0 0 0 0 0 0 0];
zone2=[0 0 0 0];
% zone1=[-45 45 -45 45 -45 45 -45 45 -45 45 -45 45 45 -45 45 -45
45 -45 45 -45];
% zone2=[-45 45 45 -45];

%%%%%%%%%%%%%%%%%%%%%%%%%%%%%%%%%%%%%%%%%%%%%%%%%%%%%%%%%%%%%%%%%%%%%%%%MATERIAL PROPERTIES FOR
RESIN%%%%%%%%%%%%%%%%%%%%%%%%%%%%%%%%%%%%%%%%%%%%%%%%%%%%%%%%%%%%%%%%%%%%%%%%
E=18854.9059054;
v=0.35;
G=10877.83033;
Alpha=1.5e-5;
%NO> OF PLY DROPED
no_of_ply_drop=16;

```

```

h_resin=tply*no_of_ply_drop;
%% S matrix for resin
S11r=1/E;
S12r=-v/E;
S66r=2*(S11-S12);
Sr=[S11r S12r 0; S12r 0 0; 0 0 S66r];
%% Q matrix for resin
Qbariso=inv(Sr);
%% THERMAL LOAD FROM ZONE 1 & 2
%% IN-PLANE forces and moment due to thermal stress
%CAL CTE in x,y direction from 1,2
for c=1:2
    if c==1
        angle=zone1;% from top to bottom
    elseif c==2
        angle=zone2;
    end
    theta=fliplr(angle); % from bottom to top
    %% h
    b=length(angle) % how many layers in the laminate
    for i=1:b+1
        h(:,i)=((-b/2)+(i-1))*tply;
    end
    h
    if c==1
        %% HEIGHT LAMINATE OF ZONE 1
        h1=b*tply
    else c==2
        %% HEIGHT OF LAMINATE OF ZONE 2
        h2=b*tply
    end
    if c==1
        NTH=zeros(3,1);
        MTH=zeros(3,1);
        %% Thermal Load for UPPER PLIES
        for k=1:b
            m = cosd(theta(k));
            n = sind(theta(k));
            Tsigma = [m^2 , n^2 , 2*m*n ; n^2 , m^2 , -2*m*n
; -m*n , m*n , m^2 - n^2];
            Tepsilon = [m^2 , n^2 , m*n ; n^2 , m^2 , -m*n ;
-2*m*n , 2*m*n , m^2 - n^2];
            Alpha_xy= inv(Tepsilon) * Alpha_12;
            Qbar = inv(Tsigma) * Q * inv(Tepsilon);
            Nth=Qbar*Alpha_xy*(h(k+1)-h(k));
            NTH=NTH+Nth;
        end
        for s=1:b
            m = cosd(theta(s));
            n = sind(theta(s));

```

```

        Tsigma = [m^2 , n^2 , 2*m*n ; n^2 , m^2 , -2*m*n
; -m*n , m*n , m^2 - n^2];
        Tepsilon = [m^2 , n^2 , m*n ; n^2 , m^2 , -m*n ;
-2*m*n , 2*m*n , m^2 - n^2];
        Alpha_xy= inv(Tepsilon) * Alpha_12;
        Qbar = inv(Tsigma) * Q * Tepsilon;
        Mth=Qbar*Alpha_xy*(h(s+1)^2-h(s)^2);
        MTH=MTH+Mth;
    end
elseif c==2
    NTH=zeros(3,1);
    MTH=zeros(3,1);
    %% Thermal Load for ZONE 2
    for k=1:b
        m = cosd(theta(k));
        n = sind(theta(k));
        Tsigma = [m^2 , n^2 , 2*m*n ; n^2 , m^2 , -2*m*n
; -m*n , m*n , m^2 - n^2];
        Tepsilon = [m^2 , n^2 , m*n ; n^2 , m^2 , -m*n ;
-2*m*n , 2*m*n , m^2 - n^2];
        Alpha_xy= inv(Tepsilon) * Alpha_12;
        Qbar = inv(Tsigma) * Q * inv(Tepsilon);
        Nth=Qbar*Alpha_xy*(h(k+1)-h(k));
        NTH=NTH+Nth;
    end

    for s=1:b
        m = cosd(theta(s));
        n = sind(theta(s));
        Tsigma = [m^2 , n^2 , 2*m*n ; n^2 , m^2 , -2*m*n
; -m*n , m*n , m^2 - n^2];
        Tepsilon = [m^2 , n^2 , m*n ; n^2 , m^2 , -m*n ;
-2*m*n , 2*m*n , m^2 - n^2];
        Alpha_xy= inv(Tepsilon) * Alpha_12;
        Qbar = inv(Tsigma) * Q * Tepsilon;
        Mth=Qbar*Alpha_xy*(h(s+1)^2-h(s)^2);
        MTH=MTH+Mth;
    end
end

if c==1
    %% Thermal Load for zone 1
    NTH1=NTH*dT
    %% Theraml Moments for zone 1
    MTH1=MTH*(dT/2)
elseif c==2
    %% Thermal Load for zone 2
    NTH2=NTH* dT
    %% Theraml Moments for zone 2

```



```

        MTH2=MTH*(dT/2)
    end

end

% % STACKING SEQUENCE FOR UPEER PLIES
% Upper_PLIES_STACK=[90 90]
% % STACKING SEQUENCE FOR LOWER PLIES
% LOWER_PLIES_STRACK=[90 90]
%% STACKING SEQUENCE FOR UPEER PLIES
Upper_PLIES_STACK=[0 0]
%% STACKING SEQUENCE FOR LOWER PLIES
LOWER_PLIES_STRACK=[0 0]
% %% STACKING SEQUENCE FOR UPEER PLIES
% Upper_PLIES_STACK=[-45 45]
% %% STACKING SEQUENCE FOR LOWER PLIES
% LOWER_PLIES_STRACK=[45 -45]
%% Laminate Thickness representation
for c=1:2
    if c==1
        angle=Upper_PLIES_STACK % from top to bottom
        %% h1
        b=length(angle) % how many layers in the laminate
        for i=1:b+1
            hu(:,i)=((-b/2)+(i-1))*tply;
        end
        hu
    elseif c==2
        angle=LOWER_PLIES_STRACK
        %% h2
        b=length(angle) % how many layers in the laminate
        for i=1:b+1
            hl(:,i)=((-b/2)+(i-1))*tply;
        end
        hl
    end
    theta=fliplr(angle); % from bottom to top
    %% equivalent height of resin
    H=h_resin/3;
    if c==1
        %% ABD MATRIX for upper plies
        A0u = zeros(3);
        B0u = zeros(3);
        D0u = zeros(3);
        for j=1:b % b= layer number
            m = cosd(theta(j));
            n = sind(theta(j));
            Tsigma = [m^2 , n^2 , 2*m*n ; n^2 , m^2 , -2*m*n
; -m*n , m*n , m^2 - n^2];

```

```

Tepsilon = [m^2 , n^2 , m*n ; n^2 , m^2 , -m*n ;
-2*m*n , 2*m*n , m^2 - n^2];
Qbar = inv(Tsigma) * Q * Tepsilon;
Au = A0u + Qbar*tply;
Bu = B0u + (1/2)*(Qbar*(H^2+(hu(j+1)^2-
hu(j)^2)));
Du = D0u + (1/3)*(Qbar*(H^3+(hu(j+1)^3-
hu(j)^3)));
A0u = Au;
B0u = Bu;
D0u = Du;
end
Au
Bu
Du
ABDu=[Au Bu;Bu Du]
INVABDu = inv(ABDu)
elseif c==2
%% ABD MATRIX for lower plies
A0l = zeros(3);
B0l = zeros(3);
D0l = zeros(3);
for j=1:b % b= layer number
m = cosd(theta(j));
n = sind(theta(j));
Tsigma = [m^2 , n^2 , 2*m*n ; n^2 , m^2 , -2*m*n
; -m*n , m*n , m^2 - n^2];
Tepsilon = [m^2 , n^2 , m*n ; n^2 , m^2 , -m*n ;
-2*m*n , 2*m*n , m^2 - n^2];
Qbar = inv(Tsigma) * Q * Tepsilon;
Al = A0l + Qbar*tply;
Bl = B0l + (1/2)*(Qbar*(hl(j+1)^2-hl(j)^2));
Dl = D0l + (1/3)*(Qbar*(hl(j+1)^3-hl(j)^3));
A0l = Al;
B0l = Bl;
D0l = Dl;
end
Al
Bl
Dl
ABDl=[Al Bl ; Bl Dl]
INVABDl = inv(ABDl)
end
end
INVABD=INVABDl-INVABDu
%%force on middle laminate
Nth_U =NTH1-NTH2
Nth_U =Nth_L
%% net force on middle laminate
Neq = Nth_U +Nth_L

```

```

Meq = Nth_U*(H+h2)+Nth_L*h2/2

H_M=h1/2-h2/2
N_PLY_DROP=NTH1-NTH2
M_PLY_DROP=N_PLY_DROP*(H)
X3= INVABD*[N_PLY_DROP;M_PLY_DROP];
STRAIN=[X3(1,1);X3(2,1);X3(3,1)]
CURVATURES=[X3(4,1);X3(5,1);X3(6,1)]

%% displacement and plot for MIDDLE LAMINATE
x = 0 : 0.0001 : 1;
y = 0 : 0.0001 : 4;
[x,y] = meshgrid(x,y);
u_o3 = STRAIN(1,1)*x + 0.5*STRAIN(3,1)*y;
v_o3 = STRAIN(2,1)*y + 0.5*STRAIN(3,1)*x;
w_o3 = -
0.5*(CURVATURES(1,1)*x.^2+CURVATURES(2,1)*y.^2 +
CURVATURES(3,1)*x.*y);
u3 = x + u_o3;
v3 = y + v_o3;
w3 = w_o3;

figure(3)
meshc(x,y,w3)

```

B-2 Code for calculating the material properties for MAT9ORT

```

clear all;
clc;
%% Young's modulus for Hexcel IM6/3501-6
E1=22000000;
E2=1300000;
E2=E3;
%% Poission's ratio for Hexcel IM6/3501-6
N12=0.3;
N23=0.35;
N31=0.35;
N21=N12;
N32=N23;
N13=N31;
%% CHECKING material stability
v=1-N12*N21-N23*N32-N31*N13-2*N21*N32*N13
%% VARIABLE FOR CALCULATING SGEAR MODULUS
NMAT=[1 -N12 -N31; -N12 1 -N32; -N13 -N23 1]

```

```

DELTA=(1/E1*E2*E3)*det(NMAT)
%% SHEAR MODULUS CALCULATION FROM MAT9ORT CARD EXPLANATION IN
HYPERMESH HELP MENU
G12=( (N21+N31*N23)/E2*E3*DELTA)

G23=( (N32+N31*N12)/E1*E3*DELTA)

G31=( (N31+N21*N32)/E3*E2*DELTA)

```

APPENDIX C
FEM file for warpage prediction

```

$$
$$ Optistruct Input Deck Generated by HyperMesh Version : 14.0.130.21
$$ Generated using HyperMesh-Optistruct Template Version: 14.0.130
$$
$$ Template: optistruct
$$
$$
$$ optistruct
$
OUTPUT,ADAMSMNF
OUTPUT,OP2,ALL
SCREEN OUT
CFAILURE(H3D,NDIV=1) = ALL
CSTRAIN(H3D,NDIV=1) = YES
DISPLACEMENT(H3D) = ALL
STRAIN(H3D) = ALL
STRESS(H3D) = YES
THERMAL(H3D) = ALL
$$$$-----$
$$ Case Control Cards $
$$$$-----$
$
$HMNAME LOADSTEP 1"loadstep1" 0
$
SUBCASE 1
 LABEL loadstep1
 SPC = 1
 TEMPERATURE(LOAD) = 2
$$$$-----
$$ HYPERMESH TAGS
$$$$-----
$$BEGIN TAGS
$$END TAGS
$
BEGIN BULK
$$

```

\$\$ Stacking Information for Ply-Based Composite Definition

\$\$

DTI UNITS 1 KG N IN S

\$HMNAME SYSTCOL 1 "systcol1"

\$HWCOLOR SYSTCOL 1 6

\$\$

\$\$ SYSTEM Data

\$\$

CORD3R 1 5960 5959 5961

\$

\$\$

\$\$ PSOLID Data

\$\$

\$HMNAME PROP 2"PROP_cover_3" 5

\$HWCOLOR PROP 2 18

PSOLID 2 2 1

\$HMNAME PROP 1"RESIN" 5

\$HWCOLOR PROP 1 6

PSOLID 1 3

\$\$

\$\$ MAT1 Data

\$\$

\$HMNAME MAT 3"RESIN" "MAT1"

\$HWCOLOR MAT 3 6

MAT1 31300000.750000.00.3 0.0457 1.5-5 350.0

\$\$

\$\$ MAT9ORT Data

\$\$

\$HMNAME MAT 2"MAT_" "MAT9ORT"

\$HWCOLOR MAT 2 5

MAT9ORT 2 2.2+71300000.1300000. 0.3 0.35 0.056

+ 2783700.321090.02997900. -5.0-7 1.5-5 350.0

\$\$

-----\$

\$\$ HyperMesh Commands for loadcollectors name and color information \$

-----\$

\$HMNAME LOADCOL 1"CONSTRAIN"

\$HWCOLOR LOADCOL 1 4

\$\$

\$HMNAME LOADCOL 2"TEMP"

\$HWCOLOR LOADCOL 2 3

ENDDATA

\$\$

-----\$\$

\$\$ Data Definition for AutoDV \$\$

-----\$\$

\$\$			
\$\$	-----	\$\$	
\$\$	Design Variables Card for Control Perturbations		\$\$
\$\$	-----	\$\$	
\$\$			
\$\$	-----	\$	
\$\$	Domain Element Definitions		\$
\$\$	-----	\$	
\$\$			
\$\$	-----	\$\$	
\$\$	Control Perturbation	\$\$	
\$\$	-----	\$\$	

References

1. Polaki, Deepak. Composite plate optimization with structural and manufacturing constraints. Diss. 2017.
2. Zhou, Ming, Raphael Fleury, and Martin Kemp. "Optimization of composite—recent advances and application." Proceeding of the 7th altair CAE technology conference. Warwickshire, United Kingdom. 2011.
3. Karim, Mohammed Rezaul. Constitutive modeling and failure criteria of carbon-fiber reinforced polymers under high strain rates. Diss. University of akron, 2005.
4. Gayen, Debabrata, and Tarapada Roy. "Hygro-thermal effects on stress analysis of tapered laminated composite beam." *International journal of composite materials* 3.3 (2013): 46-55.
5. Chamis, C. C. "A theory for predicting composite laminate warpage resulting from fabrication." (1974).
6. Akovali, Güneri, ed. Handbook of composite fabrication. Ismithers Rapra Publishing, 2001.
7. Hsiao, H. M., and I. M. Daniel. "Effect of fiber waviness on stiffness and strength reduction of unidirectional composites under compressive loading." *Composites science and technology* 56.5 (1996): 581-593.
8. Grant, Carroll. "Automated processes for composite aircraft structure." *Industrial Robot: An International Journal* 33.2 (2006): 117-121.
9. Chitwood BE, Howeth MS. "Composite tape laying machine with pivoting presser member." Patent 4627886, 6th April 1971.
10. Goldsworthy WB. "Geodesic path length compensator for composite-tape placement method." Patent US 3810,805, 14th May 1974.

11. Dirk, H-JA Lukaszewicz, Carwyn Ward, and Kevin D. Potter. "The engineering aspects of automated prepreg layup: History, present and future." *Composites Part B: Engineering* 43.3 (2012): 997-1009.
12. Wijskamp, Sebastiaan. *Shape distortions in composites forming*. University of Twente, 2005.
13. Johnson, Robert R., Murat H. Kural, and George B. Mackey. *Thermal Expansion Properties of Composite Materials*. LOCKHEED MISSILES AND SPACE CO INC SUNNYVALE CA, 1981.
14. Kappel, Erik, et al. "Spring-in and Warpage-Progress in Simulating Manufacturing Aspects." *Mechanics of Composite Materials* 29.2 (2013): 193.
15. Haynes, Robert, et al. "On plane stress and plane strain in classical lamination theory." *Composites Science and Technology* 127 (2016): 20-27.
16. Svanberg, J. Magnus. *Predictions of manufacturing induced shape distortions: high performance thermoset composites*. Diss. Luleå tekniska universitet, 2002.
17. Her, shiuh-chuan. "stress analysis of ply drop-off in composite structures." *composite structures* 57.1 (2002): 235-244.
18. Gürdal, zafer, raphael t. Haftka, and prabhat hajela. *Design and optimization of laminated composite materials*. John wiley & sons, 1999.
19. Ghiasi, hossein, et al. "optimum stacking sequence design of composite materials part ii: variable stiffness design." *composite structures* 93.1 (2010): 1-13.
20. Pagano, n. J., and r. Byron pipes. "the influence of stacking sequence on laminate strength." *journal of composite materials* 5.1 (1971): 50-57.
21. Tsai, s. W., j. C. Halpin, and n. J. Pagano. "composite materials workshop, 1968."

22. Fukunaga, Hisao, and Hideki Sekine. "Optimum design of composite structures for shape, layer angle and layer thickness distributions." *Journal of composite materials* 27.15 (1993): 1479-1492.
23. Garschke, C., et al. "Out-of-autoclave cure cycle study of a resin film infusion process using in situ process monitoring." *Composites Part A: Applied Science and Manufacturing* 43.6 (2012): 935-944.
24. Varughese, Byji, and Abhijit Mukherjee. "A ply drop-off element for analysis of tapered laminated composites." *Composite structures* 39.1-2 (1997): 123-144.
25. H Abdulhamid, C Bouvet, L Michel, J Aboissière. "Influence of internally dropped-off plies on the impact damage of asymmetrically tapered laminated CFRP." *Composites Part A: Applied Science and Manufacturing* 68 (2015): 110-120.
26. Ky, Ky. "Effect of dropped plies on the strength of graphite-epoxy laminates." *AIAA journal* 30.2 (1992).
27. Taylor, R.M., Admani, M.A., and Strain, J.M., "Comparison of Methodologies for Optimal Design of a Composite Plate under Practical Design Constraints," *Proceedings of the 55th AIAA/ASME/ASCE/AHS/ASC Structures, Structural Dynamics, and Materials Conference*, National Harbor, Maryland, 2014.
28. Flabel J.C., "Practical Stress Analysis for Design Engineers: Design and Analysis of Aerospace Vehicle Structures", *Lake city publishing company*, 1997
29. Grant, P. And Sawicki, A., "Development of Design and Analysis Methodology for Composite Bolted Joints," *Proceedings, AHS National Technical Specialists Meeting on Rotorcraft Structures*, Williamsburg, VA, October 1991

30. M. Pohlak *, J. Majak, K. Karjust, R. Küttner, "Multi-criteria optimization of large composite parts," 15th International Conference on Composite Structures, ICCS 15, porto, prt,2009.
31. Yuan, zhenyi, et al. "an analytical model on through-thickness stresses and warpage of composite laminates due to tool-part interaction." *composites part b: engineering* 91 (2016): 408-413.
32. J & j mechanic." <http://www.jjmechanic.com/process/v_bag.htm. N.p., n.d. Web. 12 aug. 2017.
33. Mats347 Composites Design And Manufacture." <<https://www.fose1.plymouth.ac.uk/sme/MATS347/MATS347C8%20autoclave.htm>>. N.p., n.d. Web. 12 Aug. 2017
34. Selvarthinam, Alex. "ME5390-002 Composite Structure: Manufacturing and repair ." Summer 2016 class lecture. Woolf Hall, UTA, Arlington. 11 June 2016 .
Lecture.